

IMPERIAL COLLEGE LONDON

DEPARTMENT OF COMPUTING

**Making Faster FEM Solvers, Faster**

MPhil Transfer Report

By

Graham Markall

Supervisors: Prof. Paul Kelly and Dr. David Ham

June 2010

## Abstract

It can be argued that producing maintainable, high performance implementations of the finite element method for multiple targets requires that they are written using a high-level *domain-specific language* (DSL). The PhD project outlined in this report is an investigation into how a DSL for the finite element method can be compiled to optimised implementations for Graphics Processing Units (GPUs).

An analysis of related literature describing the implementation of finite element methods on GPUs is presented, and it is shown that these optimisations may be concealed beneath the level of abstraction of the *Unified Form Language* (UFL), a DSL for the finite element method. Preliminary investigations involving the implementation of a high-performance GPU-based advection-diffusion solver, and a UFL compiler that generates efficient GPU codes are presented. The literature review and experiments provide a basis for future investigations towards the completion of this PhD project.

The long-term goal of this project is to integrate high-performance generated codes into Fluidity, a general-purpose computational fluid dynamics package. This will facilitate the aggressive exploitation of future manycore architectures, and reduce the complexity of further development of finite element methods.

# Contents

<b>1</b>	<b>Introduction</b>	<b>1</b>
1.1	Motivation and Outline	1
1.2	Publications and Presentations	2
1.3	Report Structure	2
<b>2</b>	<b>Background</b>	<b>3</b>
2.1	Introduction	3
2.2	Manycore Architectures	3
2.2.1	Current Hardware - NVidia Fermi	3
2.2.2	Performance Considerations	5
2.2.3	Other Architectures	5
2.2.4	Programming Languages	5
2.2.5	Remarks	6
2.3	The Finite Element Method	7
2.3.1	A Brief Overview	7
2.3.2	Boundary Conditions	8
2.4	Implementation	8
2.5	Conclusions	10
<b>3</b>	<b>Literature Review</b>	<b>11</b>
3.1	Introduction	11
3.2	The FEniCS Project and UFL	11
3.2.1	UFL Compiler Optimisations	12
3.3	The Implementation of the Finite Element Method on GPUs	13
3.3.1	Data Layout and Alignment	13
3.3.2	Mesh Reordering	14
3.3.3	Kernel Granularity and Kernel Fusions	14
3.4	Colouring and Partitioning	16
3.4.1	Oplus2	17
3.5	Algebraic Transformations	17
3.5.1	Transforming the Global Assembly Phase	17
3.5.2	Evaluation of Integral Forms by Tensor Representation	18
3.6	Related Areas	19
3.6.1	Library Generators	19
3.6.2	Acumen	21
3.6.3	Autotuning Libraries	21
3.6.4	Active Libraries	22
3.6.5	Formal Linear Algebra Methods Environment	22
3.7	Conclusions	22

<b>4 Preliminary Investigations</b>	<b>25</b>
4.1 Introduction . . . . .	25
4.2 Data Format Considerations . . . . .	25
4.3 Experiments . . . . .	26
4.3.1 CUDA and CPU Implementations and Experimental Setup . . . . .	26
4.3.2 Results . . . . .	27
4.4 Further Investigations . . . . .	29
4.5 A Prototype Compiler . . . . .	29
4.5.1 Further UFL Compiler Development . . . . .	29
4.6 Conclusions . . . . .	30
<b>5 Research Plan</b>	<b>33</b>
5.1 Introduction . . . . .	33
5.2 Work Items . . . . .	33
5.3 Potential Publications . . . . .	35
5.4 Conclusions . . . . .	36

# Chapter 1

## Introduction

This report describes a summary of the research that has been completed during the first 9 months of my PhD. This research forms a basis for further study over the next two years.

### 1.1 Motivation and Outline

Fluidity [Gorman *et al.*, 2009, Piggott *et al.*, 2009] is a computational fluid dynamics package that uses the finite element method on unstructured meshes to simulate complex models of oceans and other phenomena. It is composed of hundreds of thousands of lines of Fortran code.

The recent emergence of manycore architectures (including GPUs) as platforms that offer a large increase in computational power over traditional architectures motivates their exploitation for computational science applications. In order to make use of these architectures with Fluidity, portions of the code must be rewritten using CUDA or OpenCL, which are the languages currently available for programming these devices. However, this will require a large investment in time and effort. Additionally, the rewritten code must be tuned for each new architecture. It is also unlikely that CUDA and OpenCL will remain the languages of choice for programming future architectures; when they are replaced, it will again be necessary to rewrite large portions of Fluidity.

We note that in general the development of finite element codes in low-level languages is complicated and error prone. This process is further complicated by the fact that optimal data layouts and access patterns differ between targets, especially when execution of the code spans multiple architectures. Additionally, the optimal choice of algorithm that implements a given operation depends on characteristics of the target hardware, and even the parameters of a specific problem. To produce efficient implementations in a low-level language, developers must maintain multiple algorithm implementations for multiple targets.

It can be argued that producing maintainable high-performance implementations of finite element methods for multiple targets requires that they are written using a high-level domain-specific language. The *Unified Form Language* (UFL) [Alnæs and Logg, 2009], is one such high-level language that allows the generation of high-performance code from maintainable sources.

This PhD project is an investigation into how tools that generate efficient low-level code for GPUs from high-level specifications written in UFL may be developed and integrated into existing codebases. Part of this investigation involves determining how finite element assembly should be implemented on GPUs in order to obtain high performance. The remainder of the project involves building a UFL compiler and embedding into it the domain knowledge that enables it to generate these optimised implementations. The completion of this project will enable a large portion of Fluidity to be rewritten in UFL, allowing future architectures to be targeted more easily, and reducing the complexity of software development.

## 1.2 Publications and Presentations

A number of presentations describing the work of this project have been given outside the college. These include:

- Experiments in unstructured mesh finite element CFD using CUDA [Markall *et al.*, 2009]. This presentation was given at the 1st UK CUDA Developers' Conference, and won the prize for the best student presentation.
- Generating optimised multiplatform finite element solvers from high-level representations [Markall *et al.*, 2010b]. This presentation was given at the 8th meeting of the IFIP Working Group 2.11 on Program Generation.
- Experiments in generating and integrating GPU-accelerated finite element solvers using the Unified Form Language [Markall *et al.*, 2010a]. This presentation was given at the FEniCS '10 Conference.

The work already completed has also been published:

- Towards generating optimised finite element solvers for GPUs from high-level specifications [Markall *et al.*, 2010c]. This publication was presented at the workshop on Automated Program Generation for Computational Science<sup>1</sup> at the 10th International Conference on Computational Science.

## 1.3 Report Structure

We begin by providing background information about GPU architectures and the finite element method in Chapter 2. We examine the literature discussing the implementation of finite element methods on GPUs, and automated programming of the finite element method in Chapter 3. Practical investigations that have been completed are reported in Chapter 4. A plan for the proposed research is outlined in Chapter 5.

---

<sup>1</sup><http://www.sc.rwth-aachen.de/Events/APGCSatICCS2010/>

# Chapter 2

## Background

### 2.1 Introduction

We begin by discussing manycore architectures, in particular the NVidia Fermi architecture. This discussion serves to highlight the differences in programming each architecture, and to draw attention to the challenges that must be overcome, particularly when implementing computations that use unstructured data.

Subsequently, we introduce the finite element method and discuss how it is typically implemented on CPU architectures. This is used as a foundation to our discussions of the various implementation choices that may be made on manycore architectures in the following chapters.

### 2.2 Manycore Architectures

#### 2.2.1 Current Hardware - NVidia Fermi

*Graphics Processing Units* (GPUs) are highly-parallel architectures that have a large memory bandwidth and many *streaming multiprocessors* (SMs). Figure 2.1 shows a schematic diagram of an SM in NVidia's latest architecture, Fermi [NVidia, 2009a]. The SM may be thought of as similar to a SIMD execution unit, or a 32-lane vector processor.

There are several levels of the memory hierarchy in Fermi. We highlight the main levels that require consideration when developing code for the Fermi architecture:

**Global Memory.** A Fermi card has up to 6GB of onboard memory that is accessible by all the SMs. This memory is the slowest, with a latency of hundreds of cycles. Since this memory is separate from the memory of the host computer, data must be marshalled into this memory before computation on the GPU can begin.

**L1 Caches.** Each SM has 64KB of private cache. This cache is split into a 48KB portion and a 16KB portion. One of these portions may be assigned to a hardware-controlled cache and the other is assigned to a software-controlled cache, at the choice of the programmer. The caches can be accessed more quickly than global memory, although it has a limited number of banks, which can lead to conflicts that lower performance.

**Registers.** Each SM has 32,768 32-bit registers. These may be accessed very quickly. However, these registers are shared between potentially thousands of threads, leaving only a small number per thread.

Execution on Fermi is performed by launching individual *kernels* that are executed by many threads in parallel. These threads are grouped at various granularities, as shown in Figure 2.2. The finest grouping is referred to as a *warp*, made up of 32 threads that all share a program counter. Since these threads share a program counter, they execute in lock-step performing the same operations on individual items of data.

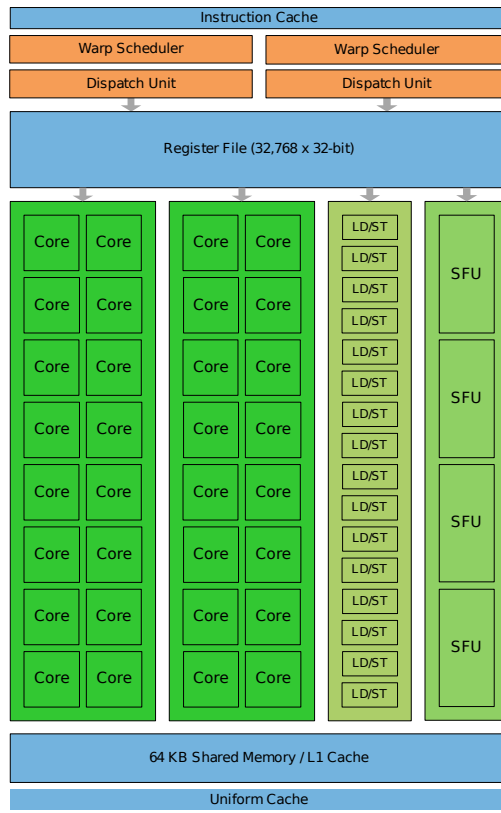


Figure 2.1: A streaming multiprocessor in Nvidia's Fermi architecture. From [Nvidia, 2009b].

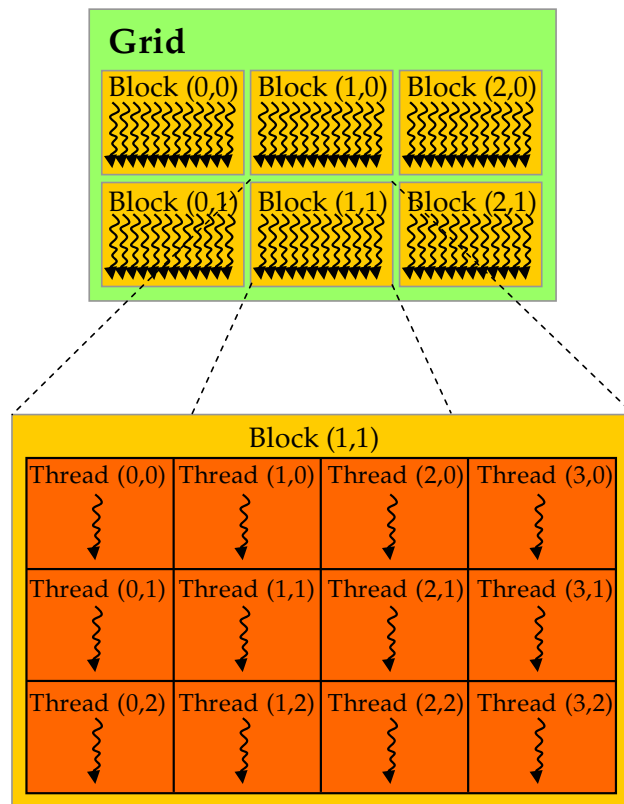


Figure 2.2: A 2D grid of 2D thread blocks. From [Nvidia, 2009a].

Several warps are grouped together to form a *block*, and the set of all blocks executing concurrently makes up the *grid*. Individual SMs are assigned a number of blocks to execute. Because each block has an affinity for one SM, communication between threads in different blocks is not possible.

### 2.2.2 Performance Considerations

Since global memory is separate from the host's memory, it is important to ensure that all computation within an inner loop is performed on the GPU. If the computation in the inner loop is divided between the GPU and the host, execution speed will be greatly reduced due to the need to constantly transfer data across the PCIe bus.

Secondly, since warps all share a single program counter, and execute the same code path concurrently, it is important that they all follow the same path of execution in the code. When threads within a warp take different paths, execution is serialised between these two paths, reducing performance.

Finally, *coalesced* memory access is needed for high memory bandwidth utilisation, and is achieved when groups of 16 threads (half of a warp) concurrently access data within a 64-byte aligned memory window. Coalescing increases the memory bandwidth utilisation because it allows multiple accesses to be transferred across the very wide data bus in a single operation. Since the threads in a half-warp are all executing the same instruction, their accesses will occur at the same time; when these accesses occur, the hardware can recognise that they fit within the window and amalgamate the accesses into a single transfer.

We have discussed the main performance considerations when writing code for the Fermi architecture. There are other considerations that are required to obtain optimum performance that are described in [NVidia, 2009a]. Often it is necessary to use tools such as the CUDA profiler [NVidia, 2010] to understand the performance of code.

### 2.2.3 Other Architectures

Although our current focus is on the Fermi architecture, it is important to note that there are other multicore and manycore architectures that are currently in use and in development. The Fermi architecture was preceded by the G80 and G200 Tesla architectures from NVidia. Although all the NVidia architectures share a programming model, their performance characteristics differ, meaning that code must be individually tuned for best performance on each device.

Other GPU architectures include AMD's Evergreen architecture [AMD, 2010], that has peak performance somewhere between that of the G200 and Fermi architectures. The Cell Processor [Gschwind *et al.*, 2006] is an interesting research platform due to its heterogeneous architectures, although it is not under further development. Intel's forthcoming Larrabee architecture [Seiler *et al.*, 2008] is heavily based on the x86 processor, and can be expected to have very different performance characteristics to GPU architectures.

### 2.2.4 Programming Languages

In order to make effective use of the GPU, programs must be designed such that the workload is decomposed into many (thousands) of data-parallel tasks that can be mapped to individual threads.

CUDA [NVidia, 2009a] is a language for programming NVidia's Tesla *Graphics Processing Units* (GPUs). It is a set of extensions to the C programming language that allows the user to define kernels for execution on the device, and includes additional keywords that are used for managing the execution of threads.

In order to give a brief overview of a CUDA kernel, we consider an example of a kernel that performs the computation  $\mathbf{y} = \alpha\mathbf{x} + \mathbf{y}$  for scalar  $\alpha$  and vectors  $\mathbf{x}$  and  $\mathbf{y}$ . A C implementation of this operation uses a loop that iterates over each element in the vectors.

```

void daxpy(double a, double *x, double *y, int n) {
    for(int i=0; i<n; i++)
        y[i] = y[i] + a*x[i];
}

```

Figure 2.3: DAXPY Kernel in C.

In order to convert this to a CUDA kernel, the work is divided between threads so that one thread computes the result for each element. This kernel is designed to be launched with as many threads as there are vector elements. Each thread calculates the offset for the element that it is assigned from the ID of its thread block, and its own ID within the block.

```

__global__ void daxpy(double a, double *x, double *y, int n) {
    int i=threadIdx.x+blockIdx.x*blockDim.x;
    if(i<n)
        y[i] = y[i] + a*x[i];
}

```

Figure 2.4: DAXPY Kernel in CUDA.

In order to standardise development for multicore architectures, the OpenCL specification [Khronos Group, 2008] has been developed. The OpenCL language shares many of the features of CUDA. However, it is designed to be compiled to executable code for a wide range of architectures, including GPUs, multicore CPUs, and the Cell processor. Since it is designed to be more flexible than CUDA in terms of supported targets, the assumptions about grids and blocks that are part of CUDA are abstracted away in OpenCL kernel code. Figure 2.5 gives an example of the daxpy kernel in OpenCL.

```

__kernel void daxpy(const double a, __global const double *x,
                    __global double* y, int n) {
    int i = get_global_id(0);
    if (i >= n)
        return;

    y[i] = y[i] + a*x[i];
}

```

Figure 2.5: DAXPY Kernel in OpenCL.

## 2.2.5 Remarks

Although it is easy to begin developing codes for GPUs and multicore systems, optimising the performance of codes on these architectures is non-trivial. It is often the case that the optimal division of work between threads and the granularity of kernels is not obvious, and various experiments must be performed in search of an optimum. Each time a new GPU architecture is released, existing codes must be re-optimised, requiring a large investment of time and effort.

Although OpenCL is portable across many targets, it is not performance portable; in the same way that different GPUs require the code to be optimised in different ways, optimising for different architectures requires further changes. Obtaining optimal performance from all the different architectures a code may be run on is not sustainable as it will require constant development effort.

Additionally, managing the marshalling of data to and from the devices, and between the various levels of the memory hierarchy places further burden on the programmer. For example, making full use of the L1 caches on Fermi requires code to be written that explicitly marshals data

at the beginning and end of execution of each kernel. Since the characteristics of the caches can vary between architectures, this adds another dimension of complexity in maintaining code for multiple targets.

## 2.3 The Finite Element Method

### 2.3.1 A Brief Overview

The finite element method is used for discretising the weak form of partial differential equations. Here we provide a brief overview of the mathematical formulation of the method - for a full treatment, see [Karniadakis and Sherwin, 1999]. We will use this explanation as a base for describing the implementation choices that may be made. The general formulation of an equation that may be discretised using the finite element method is of the form:

$$L(u) = q \quad (2.1)$$

where  $L$  is any linear differential operator,  $u$  is an independent variable, and  $q$  is a known function that does not depend on  $u$ . For example,  $L \equiv \nabla^2$  and  $q$  is the source term in Poisson's equation. Solving this equation numerically provides gives a solution  $u^\delta$ , which may not satisfy Equation 2.1 perfectly. So we have:

$$R(u^\delta) = L(u^\delta) - q \quad (2.2)$$

Here  $R$  is the *residual*, which provides a measure of the amount by which the numerical solution does not satisfy the original problem. In the ideal case,  $R = 0$ , and the numerical solution is the exact solution, so we must try to eliminate this term. However, requiring the numerical solution to be exact makes it too difficult to find a solution to most problems. If we are prepared to tolerate some inaccuracy, we can transform the system to weaken the definition of equality. First, we multiply the equation by an arbitrary *test* function,  $v$ , and then integrate over the whole domain,  $\Omega$ , giving:

$$\int_{\Omega} vR(u^\delta) \, dX = \int_{\Omega} vL(u^\delta) \, dX - \int_{\Omega} vq \, dX \quad (2.3)$$

Now, we assume that  $R = 0$ , which makes the integral on the left-hand side disappear, leaving us with:

$$\int_{\Omega} vL(u^\delta) \, dX = \int_{\Omega} vq \, dX \quad (2.4)$$

This form is known as the *integral form* of Equation 2.1. The left-hand side of this equation defines an inner product between the test function  $v$  and the *trial function*  $L$ , and therefore can be considered as a projection of  $v$  into  $L$ . Because the function  $q$  is known, we can evaluate the right-hand side, and then compute the aforementioned projection to give  $u^\delta$ . This projection is known as the *Galerkin Projection*.

In order to evaluate the right-hand side and the projection at discrete points (as is necessary on a computer with finite memory and processing power), the integral form must be discretised. The discretisation allows us to represent functions in the test and trial spaces as a linear combination of basis functions. For example, we represent the solution as  $u^\delta = \sum_{i=1}^N \hat{u}_i \Phi_i$  where  $N$  is the number of functions in the basis for this space, and  $\hat{u}_i$  is the  $i$ -th coefficient of the  $i$ -th basis function,  $\Phi_i$ . The basis functions are chosen so that

$$\Phi_i(x_i) = 1, \text{ and } \forall k : i \neq k, \Phi_i(x_k) = 0 \quad (2.5)$$

where  $x_i$  is the  $i$ -th node in a set of nodes placed at discrete points in the domain. Although a wide variety of choices of basis function are possible, we consider a simple basis for a 1D domain. We can define the basis functions as follows:

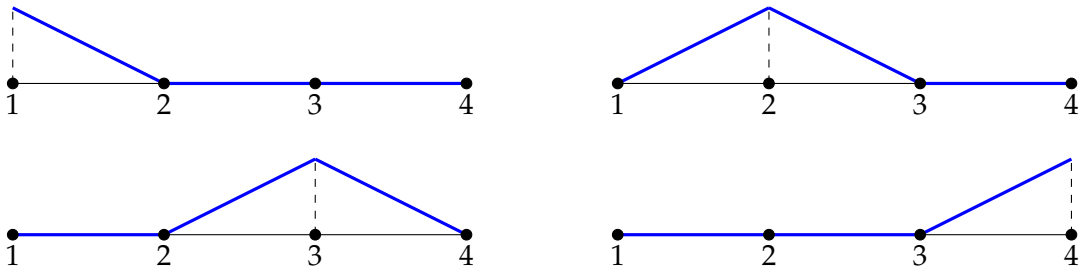


Figure 2.6: A piecewise continuous linear basis over a one-dimensional domain with four nodes and three elements.

$$\Phi_i = \begin{cases} \frac{x-x_{k-1}}{x_k-x_{k-1}} & \text{if } x \in [x_{k-1}, x_k] \\ \frac{x_{k+1}-x}{x_{k+1}-x_k} & \text{if } x \in [x_k, x_{k+1}] \\ 0 & \text{otherwise.} \end{cases} \quad (2.6)$$

This is a piecewise linear basis. An example of this basis for a four-node domain is shown in Figure 2.6

Having decided on a discretisation, we may now proceed to evaluate the integrals on both sides of Equation 2.4. The result of this process, a linear system of equations

$$A\mathbf{x} = \mathbf{b} \quad (2.7)$$

is assembled, in which the matrix  $A$  is derived from the LHS and the vector  $\mathbf{b}$  is derived from the RHS of the weak form. The solution to this system of equations,  $\mathbf{x}$ , is the solution to the discretised problem.

### 2.3.2 Boundary Conditions

Often boundary conditions must be enforced in order for there to be a unique solution to a differential equation. Boundary conditions are usually one of two kinds:

**Dirichlet.** These specify the exact value of a function at a boundary node. An example of a Dirichlet boundary condition is the no-slip condition,  $\mathbf{u} = 0$ , which states that the velocity of a fluid is zero at a boundary, and the free-slip condition,  $\mathbf{u} \cdot \mathbf{n} = 0$ , which states that fluid moves freely along a boundary, but not through it.

**Neumann.** These specify the value of the derivative of a function at a boundary node. An example of a Neumann boundary condition is the do-nothing boundary condition,  $\frac{\partial \mathbf{u}}{\partial \mathbf{X}} = 0$ , which prescribes free flow out of the domain.

The implementation of boundary conditions in the finite element method involves a similar process to that for the entire domain. In evaluating boundary condition contributions, only the edges of the domain are considered, which requires computations in a domain of dimension that is one lower than the whole domain. For example, in a 2D domain, 1D line integrals are evaluated over the boundaries, and in a 3D domain, 2D surface integrals are evaluated over the boundaries.

## 2.4 Implementation

Solving a partial differential equation with a time-varying solution using the finite element method typically consists of the following phases for each timestep:

**Local Assembly.** For each element  $i$  in the domain, an  $N_e \times N_e$  matrix,  $\mathbf{M}_i^e$ , and an  $N_e$ -length vector,  $\mathbf{b}_i^e$ , are computed, where  $N_e$  is the number of nodes per element. These are referred to as



Figure 2.7: *Left*: A 1D domain decomposed into two elements ( $\Omega^i$ ). *Right*: Local node numbering of individual elements.

*local* matrices and vectors. Computing these matrices and vectors usually involves the evaluation of integrals over the elements using Gaussian quadrature. In most implementations, every element has the same number of nodes.

**Global Assembly.** The local matrices,  $\mathbf{M}^e$ , and vectors,  $\mathbf{b}^e$ , are used to form a *global matrix*,  $\mathbf{M}$ , and *global vector*,  $\mathbf{b}$ , respectively. This process couples the contributions of elements together.

**Solution.** The system of equations  $\mathbf{M}\mathbf{x} = \mathbf{b}$  is solved for  $\mathbf{x}$ , often using an iterative method, which requires computation of the *sparse matrix-vector product* (SpMV)  $\mathbf{y} = \mathbf{M}\mathbf{v}$ .

We shall examine the global assembly phase, which consists of performing the following computations:

$$\mathbf{M} = \mathcal{A}^T \mathbf{M}^e \mathcal{A} \quad (2.8)$$

$$\mathbf{b} = \mathcal{A}^T \mathbf{b}^e \quad (2.9)$$

where  $\mathcal{A}$  is a matrix mapping the local node numbers of each element to the global node numbers,  $\mathbf{M}^e$  is a block-diagonal matrix whose  $i$ -th block is  $\mathbf{M}_i^e$ , and  $\mathbf{b}^e$  is a vector of stacked  $\mathbf{b}_i^e$ . We shall examine algorithms that can be used to implement these computations, as the optimal choice of algorithm depends on the target hardware. Consider a two-element, three-node decomposition of a 1-dimensional domain (see Figure 2.7). In this example, the matrices and vector are:

$$\mathcal{A} = \begin{bmatrix} 1 & & \\ & 1 & \\ & & 1 \end{bmatrix} \quad \mathbf{M}^e = \begin{bmatrix} m_{11}^1 & m_{12}^1 & & \\ m_{21}^1 & m_{22}^1 & & \\ & & m_{11}^2 & m_{12}^2 \\ & & m_{21}^2 & m_{22}^2 \end{bmatrix} \quad \mathbf{b}^e = \begin{bmatrix} b_1^1 \\ b_2^1 \\ b_1^2 \\ b_2^2 \end{bmatrix}$$

where  $m_{ij}^e$  is the  $i, j$ -th term of the local matrix for element  $\Omega^e$ , and  $b_i^e$  is the  $i$ -th term of the local vector for element  $\Omega^e$ . The structure of  $\mathcal{A}$  arises from the geometry of the elemental decomposition of the domain.

It is often inefficient to compute the matrix multiplications described in Equations 2.8 and 2.9 on traditional architectures due to the sparsity of  $\mathcal{A}$ . The *Addto* algorithm is usually more efficient. To describe this algorithm, we first define an array,  $\text{map}[e][i]$ , that maps the local node  $i$  of the element  $e$  to a global node number. In our example, the array is defined as:

$$\text{map}[1][i] = \begin{bmatrix} 1 \\ 2 \end{bmatrix} \quad \text{map}[2][i] = \begin{bmatrix} 2 \\ 3 \end{bmatrix}$$

Algorithms 1 and 2 describe the *Addto* algorithm for computing  $\mathbf{M}$  and  $\mathbf{b}$ . Intuitively, terms of the local matrix (or vector) of each element are summed into particular terms in the global matrix (or vector) depending on the node numbers of the element.

These algorithms are massively data-parallel, as iterations of all the loops can be executed independently of others. Although this appears to make them ideal for implementing on GPU architectures, there are two issues. First, data races occur if threads concurrently update the same term of the global matrix. Costly atomic operations must be used to ensure correctness. Second,  $\mathbf{M}$  is often stored using a format such as *compressed sparse row* (CSR). Finding the location in memory of a particular term requires a bisection search of the sparsity structure of the matrix, leading to uncoalesced accesses and control flow divergence within warps.

---

**Algorithm 1:** Addto for global matrix assembly.

---

```
1 M = 0 ;
2 foreach Element e do
3   for i  $\leftarrow$  1 to  $N_e$  do
4     for j  $\leftarrow$  1 to  $N_e$  do
5       M[map[e][i], map[e][j]] +=  $\mathbf{M}^e[i, j]$  ;
```

---

---

**Algorithm 2:** Addto for global vector assembly.

---

```
1 b = 0 ;
2 foreach Element e do
3   for i  $\leftarrow$  1 to  $N_e$  do
4     b[map[e][i]] +=  $\mathbf{b}^e[i]$  ;
```

---

## 2.5 Conclusions

We have examined the Fermi architecture, and briefly discussed other multicore and manycore architectures. These architectures bring considerable challenges when developing unstructured codes, particularly due to their requirements for accessing data in a structured fashion. Furthermore, the need to marshal data onto and off the device and through the various levels of their memory hierarchy further complicates code, and reduces its portability.

The finite element method is typically implemented using unstructured data and indirect accesses, which are unlikely to be efficient when implemented on manycore architectures. In the following chapter, we will examine some of the techniques that have been used to overcome these issues and improve performance.

# Chapter 3

## Literature Review

### 3.1 Introduction

As we have seen in the previous chapter, the implementation of finite element methods on many-core architectures is challenging. In this chapter we examine how these issues have been tackled in implementations that are described in the literature. In particular we will examine data structures, partitioning of the data and the tasks between threads, and strategies for avoiding contention between parallel threads.

We begin by discussing the FEniCS project, which has worked towards the automation of the finite element method. The outputs of the FEniCS project, in particular the Unified Form Language, provide an appropriate level of abstraction for the finite element method that makes it easy to develop and maintain codes, and allows flexible choice in the low-level implementation and a choice of optimisations to be made. Presently the FEniCS project tools provide support for CPU architectures only. We discuss how this work may be further extended to support the generation of CUDA/OpenCL, using alternative data structures and algorithms that are more efficient on manycore architectures.

We also examine alternative algorithms for implementing the finite element method, and discuss the impact that this has had on the performance of simulations with varying parameters on CPU architectures. These algorithms can also be implemented on GPU architectures, but their performance can be expected to vary differently in relation to the problem parameters.

Finally, we examine techniques that have been successfully used to generate optimised code from high-level specifications in other areas of computational science. These domains include signal processing, cyber-physical systems, and tensor contraction computations for quantum chemistry. We discuss how these techniques may be applied in the generation of finite element solvers from high-level specifications.

### 3.2 The FEniCS Project and UFL

There are a number of tools that are designed to make the implementation of finite element methods easier. These include libraries such as deal.II [Bangerth *et al.*, 2007], Diffpack [Langtangen, 2003], Sundance [Long, 2003], as well as the XFEM library [Bordas *et al.*, 2007] for the extended finite element method [Moes *et al.*, 1999]. Domain-specific languages such as Analysa [Bagheri and Scott, 2004], FreeFEM [Hecht *et al.*, 2005], GetDP [Dular and Geuzaine, 2005] and Hedge [Klöckner, 2010] have also been developed.

We focus our discussion on the FEniCS project [Logg, 2007], as the tools from this project provide complete automation of the finite element method. The main environment, DOLFIN [Logg and Wells, 2010] is used to define and solve a Partial Differential Equation (PDE) problem, allowing specification of the PDE, boundary conditions, the mesh, and timestepping. The Unified Form Language is used for the specification of variational forms.

For a complete UFL reference, see [Alnæs and Logg, 2009]. We examine UFL with an example that shows how it can be used to describe the assembly and solution of a partial differential

equation. Poisson's Equation, and a weak form are:

$$\nabla^2 u = f \quad (3.1)$$

$$\int_{\Omega} \nabla v \cdot \nabla u \, dX = \int_{\Omega} vf \, dX \quad (3.2)$$

We assume the boundary condition  $\int_{\partial\Omega} v \nabla u \cdot \mathbf{n} \, ds = 0$  to simplify the example. Figure 3.1 gives the UFL code for the assembly and solution of the weak form. Lines 1 and 2 instruct the compiler that  $v$  and  $u$  are test and trial functions, which is known from the mathematical formulation of the problem. The known function  $f$  is specified as a function of coordinates within the domain.  $A$  and  $RHS$  specify the left- and right-hand sides of Equation 3.2. The final line specifies that these forms are to be assembled into a linear system, which is solved to find the solution to the problem. The `solve` keyword is an addition to UFL, which is usually provided by tools that are part of the FEniCS project.

```
v=TestFunction(P)
u=TrialFunction(P)
f=Function(P, sin(x[0])+cos(x[1]))
A=dot(grad(v),grad(u))*dx
RHS=v*f*dx
P = solve(A,RHS)
```

Figure 3.1: UFL code for the assembly and solution of Poisson's Equation.  $P$  is assumed to be some finite element space over a mesh.

Note that UFL provides a means to give a complete specification of how the problem may be solved using the finite element method, yet contains no implementation-specific information. This provides the flexibility to generate code for multiple architectures, using alternative algorithms - the code is effectively "future-proofed". Compare this with a direct implementation in a low-level language, for which it is difficult to transform the data layout or implementation algorithm. The UFL compiler eventually commits to specific aspects of the low-level implementation during one or more of its passes.

Although the example covers the specific forms in Poisson's equation, the UFL formalism is sufficiently flexible to allow the representation of any multilinear form. It can therefore be used to describe the finite element formulation of any PDE.

Targeting a new platform is accomplished by the development of a new compiler backend, without modifying the UFL sources. This allows the concerns of different developers to be separated: the work of mathematicians who test and implement new schemes is decoupled from the work of those whose concern is the low-level implementation of codes. This separation eases the development of finite element codes by eliminating a large proportion of the repetitive and error-prone tasks that are usually required. The generated code can be better optimised than handwritten code, as optimisations often cut across the boundaries of the abstractions required for developing software in low-level languages.

### 3.2.1 UFL Compiler Optimisations

As a UFL Compiler is given a declarative specification rather than an imperative one, it is free to make choices about how the generated code should implement the specification in order to optimise performance. We shall consider an example of one of the choices the compiler may make. First, we point out that it is not always efficient to assemble a matrix whenever the assignment of a bilinear form is encountered. Instead, the best course of action depends on how the resulting matrix is subsequently used. For example, consider a portion of the assembly of a diffusion scheme:

```

M=p*q*dx          # Mass matrix
rhs=action(M+0.5*d, t) # Right-hand side vector
A=M-0.5*d        # Left-hand side matrix

```

In this example the mass matrix is not used as a matrix of coefficients in a system of equations, but is only used as an intermediary matrix for the construction of the matrix  $A$ , and the right-hand side vector. Assembling a full sparse matrix for  $M$  will be very costly in terms of memory usage, and possibly in terms of computation required to construct the matrix sparsity pattern.

Since the mass matrix is not directly required, an efficient schedule for executing this code may consist of fusing the loops that assemble the right-hand side vector and the matrix. After this optimisation, the local matrices that make up the mass matrix may be assembled for each element in the mesh at each iteration of the loop - this local matrix may then be used to compute the action of the mass matrix on the local vector, and also added into the local matrix for  $A$ . At the end of an iteration of the loop, the mass matrix is no longer required, and can be freed. To summarise the effect of this optimisation, it avoids a *Sparse Matrix-Vector* (SpMV) product being computed for a very large sparse matrix, replacing it with many small, dense matrix-vector multiplications.

Whether it is more efficient to fully assemble the mass matrix or to only ever assemble its local matrices depends upon the target architecture. This example demonstrates that there is an optimisation space to be explored, and that differs between architectures. Furthermore, the user of UFL need not consider this optimisation space as it is abstracted away.

There are further examples of optimisations that can be made without modifying the UFL sources. Other optimisations that we describe throughout the remainder of this chapter can be implemented in a UFL compiler and effectively hidden from the end user. These optimisations affect aspects of the code including:

- The structure of the assembly loop. This structure determines the number of elements the loop operates on concurrently, how the kernels are fused.
- Changes to the layout of data structures representing the mesh and associated data, and its alignment.
- Partitioning the computational workload and re-ordering of computations in order to avoid inefficient operations.
- The algorithms used to implement the global assembly phase.

### 3.3 The Implementation of the Finite Element Method on GPUs

There are a number of implementations of finite element methods on GPUs that are described in the literature. These implementations have been applied to fields including earthquake modelling [Komatitsch *et al.*, 2009, Komatitsch *et al.*, 2010], electromagnetic scattering [Klöckner *et al.*, 2009, Klöckner, 2010], hyperelastic material simulation [Filipovic *et al.*, 2009a, Filipovic *et al.*, 2010], and surgical simulation [Miller *et al.*, 2007, Taylor *et al.*, 2007, Taylor *et al.*, 2008, Comas *et al.*, 2008]. Investigations into the implementation of the local assembly phase have shown that performance on the GPU can vary between problems with various parameters [Maciol *et al.*, 2010]. Some implementations of multigrid solvers on GPUs are used to accelerate the solution phase of the finite element method, including [Turek *et al.*, 2010, Göddeke *et al.*, 2009]. However, we exclude discussions of linear solvers from our review as they do not make up part of the finite element assembly process. In the remainder of this section we examine the techniques used to implement the finite element method efficiently on GPU architectures.

#### 3.3.1 Data Layout and Alignment

One approach [Klöckner *et al.*, 2009] described in the literature involves partitioning the mesh into small chunks that can be co-operatively loaded into shared memory by a thread block, before computation proceeds on this data. Since data is reused between elements that share a face, it is more

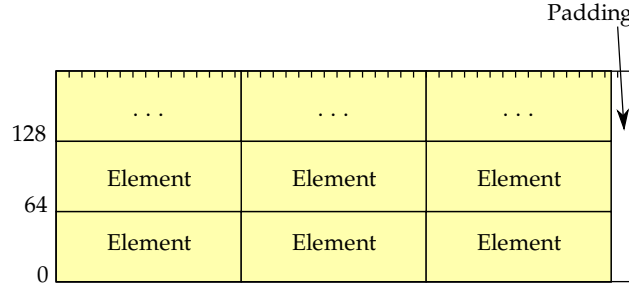


Figure 3.2: Data layout for threads to co-operatively load element data from a small partition into shared memory. From [Klöckner *et al.*, 2009].

efficient to try to load in a set of elements that share as many faces as possible. This can be achieved by partitioning the mesh into many very small partitions that consist of the maximum number of elements that can be loaded into shared memory. It has been reported that standard partitioning tools (such as [Karypis and Kumar, 1998]) fail to work efficiently for creating such partitions, as they are designed with partitioning a mesh into fewer, larger sets in mind [Klöckner *et al.*, 2009]. Instead, a simple greedy partitioning algorithm has been shown to be effective for this purpose.

Given the variety of finite element types [Raviart and Thomas, 1977, Brezzi *et al.*, 1985, Brezzi *et al.*, 1987, Nedelec, 1980, Crouzeix and Raviart, 1973] and the various orders of their polynomial bases, it will often be the case that the number of floating-point values required for representing the data for a single element will not be a multiple of 16 (the most amenable size for achieving coalescing), it is necessary to consider the size of the elements when determining their data layout. A scheme that allows coalescing involves packing together element data for several elements that require less than 64 bytes. The remaining space from the end of the element data up to 64 bytes is then filled with padding. When using this data structure, half-warps can co-operate to load element data. Although some space and bandwidth is wasted, this scheme avoids the need for complicated calculations for loading the correct data for each element whilst still obtaining coalescing. This scheme will have the poorest performance in the case where the element data requires just over 8 floats, since it will not be possible to fit another element's data within the same 64 bytes, so the wastage due to padding will be close to 50%. Figure 3.2 shows an example of this scheme for element data that requires 5 floats per element. Three elements can be packed together with 4 bytes (1 float) for padding.

### 3.3.2 Mesh Reordering

The Reverse Cuthill-McKee algorithm [Cuthill and McKee, 1969] reorders the nodes of a mesh so that the non-zero terms of the corresponding matrix are pushed as closely towards the main diagonal as possible. Although this does not make the finite element assembly run any faster, it can increase the speed of the SpMV operation in the solver due to the increased locality in the source vector. Figure 3.3 shows the global matrix for a mesh before and after the reordering is performance.

On CPU architectures, the reordering has a beneficial effect since CPU caches are large. The reordering has been implemented in a GPU solver [Göddeke *et al.*, 2005], although it made little difference to the performance due to the lack of a hardware-managed cache on the platform upon which it was tested (the NVidia G80). Since the Fermi architecture has a small hardware-controlled cache on each SM, it is expected that this reordering will have some performance benefit.

### 3.3.3 Kernel Granularity and Kernel Fusions

It is relatively straightforward to decide how to parallelise very fine-grained and very coarse-grained operations on GPUs. For the fine-grained operations, using a single thread per output is usually sufficient. Coarse-grained operations may be implemented by using an entire thread block

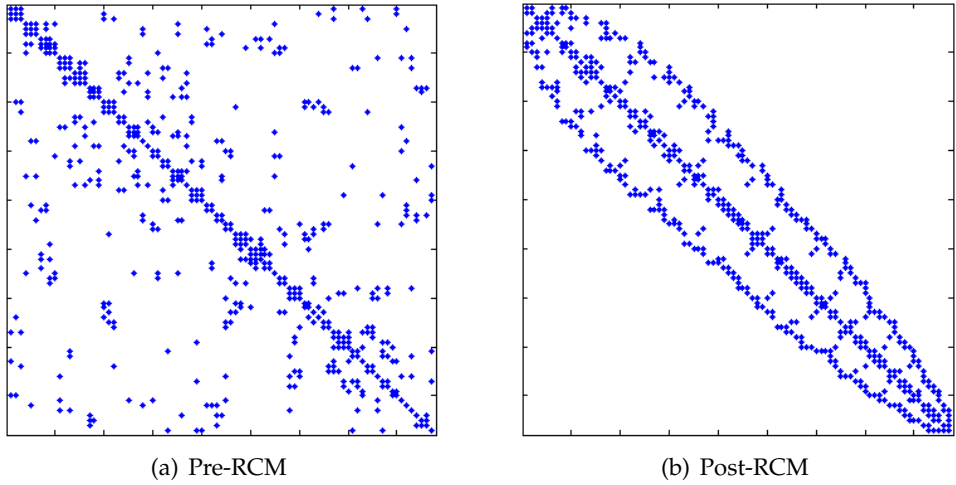


Figure 3.3: A sparse matrix before and after Reverse Cuthill-McKee reordering.

(consisting of between 64 and 1024 threads) to produce a single output. It has been identified in [Filipovic *et al.*, 2009a] that there are a number of operations in finite element assembly that do not easily fit into either of these categories, and are termed *medium-grained* operations. These operations typically require between 3 and 12 threads to compute a single output efficiently.

The granularity of operations presents an issue due to the tradeoff between kernel code size and intermediate storage size. It is desirable to perform as many operations as possible in a single kernel (as opposed to spreading operations over multiple kernels), reducing the need for intermediate storage of values in global memory. Because of the large data-parallelism of operations on the GPU, many intermediate values must be stored between invocations of different kernels, consuming a significant amount of memory bandwidth and space. However, as kernel code size increases, the number of registers required per thread also increases. Since registers are limited, larger and more complex kernels have to be executed using fewer concurrent threads, which reduces performance. Choosing the boundaries between kernels in the implementation of an operation is a non-trivial task.

It has been outlined that splitting each operation into a single kernel is not the optimal choice - experimental results in [Filipovic *et al.*, 2009a] show that fusing some operations increases performance, due to the aforementioned reduction in memory bandwidth usage. Regarding the granularity of operations, it is noted that fusing two operations of differing granularity produces a single kernel, a subset of whose threads are idle for part of the execution. Although some inefficiency has been introduced, can be a worthwhile trade-off, due to a reduction in the global memory accesses.

Figure 3.4 gives an example of the fusion of kernels of differing granularity. In this example, operation  $O_3$  reads in the intermediate results written out by  $O_1$ . Therefore, operations  $O_1$  and  $O_3$  can be rearranged and fused. The portion of the new kernel from  $O_3$  will leave two thirds of the threads idle. However, a write and read of intermediate results between these two kernels is eliminated.

A general methodology for producing an implementation with fusions is described in [Filipovic *et al.*, 2009a]. Here, we attempt to summarise the basic step of this methodology, referred to as the *decomposition-fusion scheme*:

1. Produce an implementation that is made up from a set of kernels that each perform a single operation. This implementation can be considered the fully-unfused implementation.
2. Determine which kernels to fuse. There is presently no concrete strategy for making this choice. The authors determine which kernels should be fused by benchmarking each of the individual kernels. Two kernels  $K_1$  and  $K_2$  may be considered candidates for fusion if:
  - $K_1$  produces intermediate results that are consumed by  $K_2$ .

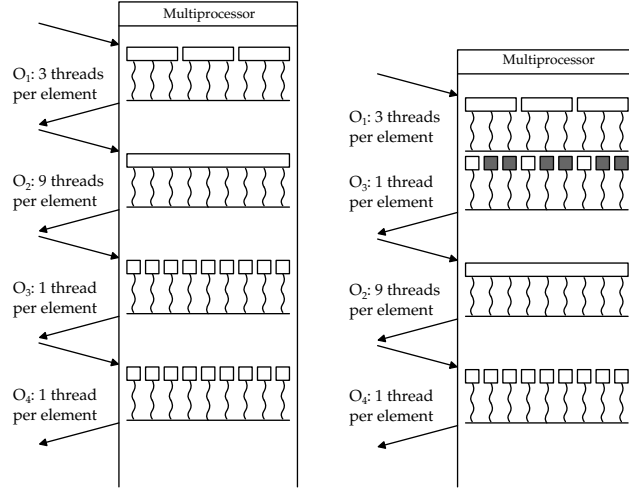


Figure 3.4: Fusing kernels of different granularities. *Left*: Unfused kernels store results in global memory. *Right*: One pair of kernels is fused. From [Filipovic *et al.*, 2009b].

- At least one of the kernels has high bandwidth utilisation and low computational intensity (in terms of GFLOPS/sec).

3. Create a new implementation in which the fusion candidates are fused.
4. Steps 2 and 3 may be repeated, until there are no fusion candidates.

Although this scheme can be used to produce implementations with a reasonable choice of fusions, there are several problems. Producing hand-implementations of the unfused implementation is quite tedious. The criteria for finding fusion candidates are not well-defined. Furthermore, producing the implementations of the fused kernels will be a tedious and error-prone manual process. It is concluded that although it is necessary to search for an optimal fusion combination to obtain the highest performance on GPU architectures, it would be highly desirable to automate this process. The decomposition-fusion scheme will be impossible to implement practically in a general-purpose compiler, as it will be too difficult to perform an analysis that provides enough information to automate the fusion. However, a compiler for a domain-specific language can be made to produce a variety of fused and unfused kernels. The choice of which kernels are the optimal ones may be guided by the development of a performance model, or by a profile-guided algorithm.

### 3.4 Colouring and Partitioning

Due to the parallel operation of the GPU, it is inevitable that there will be some contention when writing data. For example, if two elements share a node, the threads performing computation for each of these elements will both need to update the same location. In order to prevent data races, techniques that can be used include the use of atomic operations, or colouring schemes.

The CUDA and OpenCL programming models provide support for certain atomic operations that can be used to implement atomic arithmetic operations on floating point numbers. Although these operations ensure consistency, they can have a large impact on performance.

Colouring schemes may be used to remove the need for atomic operations, by ensuring that entities whose updates may be in conflict have different colours. The execution proceeds in parallel over each colour, but each colour is processed sequentially. This prevents any contention.

It is usually sufficient to perform the colouring using the Welch-Powell algorithm [Lipschutz and Lipson, 1997], which is a simple greedy algorithm, and is detailed in Algorithm 3. This algorithm is often sufficient as it is guaranteed to colour a graph with chromatic number  $\Delta$  using  $\Delta + 1$  colours.

---

**Algorithm 3:** The Welch-Powell algorithm for colouring a graph  $G$ . From [Lipschutz and Lipson, 1997].

---

- 1 Order the vertices of  $G$  according to decreasing degrees ;
- 2 Assign the first colour  $C_1$  to the first vertex and then, in sequential order, assign  $C_1$  to each vertex which is not adjacent to a previous vertex which was assigned  $C_1$  ;
- 3 Repeat Step 2 with a second colour,  $C_2$  and the subsequence of non-coloured vertices ;
- 4 Repeat Step 3 with a third colour,  $C_3$ , then a fourth colour,  $C_4$ , and so on until all vertices are coloured.

---

The use of a colouring scheme for avoiding atomic operations has been successfully applied in the development of a large-scale earthquake model written in CUDA [Komatitsch *et al.*, 2009, Komatitsch *et al.*, 2010].

### 3.4.1 Oplus2

OPlus2 [Giles, 2010] is a general framework for programming unstructured mesh applications on GPUs that is currently under development. We draw attention to the proposed colouring scheme for avoiding atomic operations, in which the colouring is performed at two levels:

- In the first level of colouring, a partitioning of the mesh into chunks that are small enough to be loaded into shared memory is made. These partitions are coloured such that no two adjacent partitions share a colour. This allows chunks of the mesh to be loaded into shared memory and computed over by concurrently operating threads, without the risk of contention. A separate kernel invocation is used for each different colour of partition.
- The edges within partitions are also coloured, since OPlus2 performs computations on an edge-by-edge basis, rather than a node-by-node basis. The colouring for each partition is independent of the colourings in other partitions. This colouring is used within the execution of one thread block on the chunk in shared memory. Executing kernels loop over the colours within the partition, to ensure that there is no contention between threads within a block.

It is expected that a similar 2-level scheme may be applied on a node-by-node basis to a mesh in order to perform computations on data in shared memory in a finite element method implementation in CUDA. However, the colouring is not strictly necessary in combination with the partitioning if the Local Matrix Approach to the Global Assembly phase is adopted (See Section 3.5.1 below).

## 3.5 Algebraic Transformations

The finite element method can be thought of as the composition of various algebraic operations on tensors [Kay, 1988]. It is possible to make transformations using algebraic operations in order to derive equivalent formulations of a method. These transformations can increase the efficiency of the method, either by reducing the operation counts, or by generating algorithms that are more amenable to the target hardware.

In this section, we examine two transformations that are discussed in the literature; it is hypothesised that these transformations are just two of a large number of possibilities that may be generated, and that each of the possible implementations will have different performance characteristics on different architectures.

### 3.5.1 Transforming the Global Assembly Phase

It was highlighted in Section 2.4 that the Addto algorithm is unlikely to be efficient on the GPU due to its indirect accesses of data structures. Here we describe how the formulation of Equation

2.8 (representing the Global Assembly phase) may be transformed to avoid the use of the Addto algorithm.

An alternative algorithm, referred to as the *Local Matrix Approach* (LMA), is derived by noting that the only use of  $\mathbf{M}$  is for computation of the product  $\mathbf{M}\mathbf{v}$  in the solution phase. We omit the global assembly of  $\mathbf{M}$  (Equation 2.8) altogether, and when computation of  $\mathbf{y} = \mathbf{M}\mathbf{v}$  is required, the following computation is performed:

$$\mathbf{y} = \left( \mathcal{A}^T (\mathbf{M}^e (\mathcal{A}\mathbf{v})) \right) \quad (3.3)$$

This transformation involves making use of the associativity of matrix-matrix multiplication to transform the chain matrix multiplication of Equation 2.8 and the Matrix-vector product  $\mathbf{M}\mathbf{v}$  into the three matrix-vector products of 3.3. It is not possible to avoid the assembly of  $\mathbf{b}$ , as it is explicitly required by the solver. However, we can eliminate the use of the Addto algorithm by computing the matrix-vector product  $\mathbf{b} = \mathcal{A}^T \mathbf{b}^e$  using an SpMV kernel.

We note that the Local Matrix Approach uses more memory bandwidth and computations than the Addto algorithm. However, this increase in operations may be amortised by the reduction in the use of inefficient memory accesses required by the Addto Algorithm. It has been shown in [Vos *et al.*, 2009] and [Cantwell *et al.*, 2010] that the Local Matrix Approach is more efficient than the Addto algorithm for certain polynomial bases when solving two- and three-dimensional problems in CPU implementations.

### 3.5.2 Evaluation of Integral Forms by Tensor Representation

The FEniCS Form Compiler [Kirby and Logg, 2006] makes use of algebraic rearrangements to optimise computations in the finite element method. Some of these optimisations are described in [Logg, 2007]. In this subsection we reproduce the workings of one of the simpler optimisations based on an algebraic transformation. This optimisation reduces the number of operations required when evaluating integrals using Gaussian quadrature. This is achieved by making a change that allows more of the computational work to be performed on the reference element. This reduces the work needed to transform the solution from the reference element to the physical element. Since the evaluation over the reference element is only performed once, whereas the transformation is performed for every element, this optimisation greatly reduces the computational cost of the overall computation.

We consider a transformation that may be applied when the mapping from the reference element to the physical element is affine. We consider a Laplacian form that may be evaluated using Gaussian quadrature as follows:

$$M_K^e[i, j] = \int_{\Omega^K} \nabla v \cdot \nabla u \, dX = \sum_{q=1}^{N_q} \sum_{\alpha=1}^{N_{dim}} w_q \frac{\partial \phi_i}{\partial X_\alpha}(\xi_q) \frac{\partial \phi_j}{\partial X_\alpha}(\xi_q) |J^K| \quad (3.4)$$

where  $w_q$  is a quadrature weight,  $J^K$  is the Jacobian of the transformation from reference space to physical space, and  $\phi$  is a basis function in physical space. In order to derive the form that performs the transformation by a tensor contraction, we first write the dot product in the integral in terms of its components:

$$M_K^e[i, j] = \int_{\Omega^K} \nabla v \cdot \nabla u \, dX = \int_{\Omega^K} \sum_{\alpha=1}^{N_{dim}} \frac{\partial \phi_i}{\partial X_\alpha} \frac{\partial \phi_j}{\partial X_\alpha} \, dX \quad (3.5)$$

Next, we can make a change of variables from the physical coordinates to the coordinates on the reference cell, giving:

$$M_K^e[i, j] = \int_{\Omega^K} \sum_{\alpha=1}^{N_{dim}} \sum_{\beta_1=1}^{N_{dim}} \frac{\partial \xi_{\beta_1}}{\partial X_\alpha} \frac{\partial \Phi_i}{\partial \xi_{\beta_1}} \sum_{\beta_2=1}^{N_{dim}} \frac{\partial \xi_{\beta_2}}{\partial X_\alpha} \frac{\partial \Phi_j}{\partial \xi_{\beta_2}} |J^K| \, dX \quad (3.6)$$

where  $\xi$  is a coordinate on the reference cell, and  $\Phi$  is a basis function on the reference cell. Since the mapping from the reference element to the physical element is affine, the sums  $\sum_{\beta}^{N_{dim}} \frac{\partial \xi}{\partial X}$  and the determinant  $|J^K|$  are constant throughout the element, and can be moved outside the integral:

$$M_K^e[i, j] = |J^K| \sum_{\alpha=1}^{N_{dim}} \sum_{\beta_1=1}^{N_{dim}} \frac{\partial \xi_{\beta_1}}{\partial X_{\alpha}} \sum_{\beta_2=1}^{N_{dim}} \frac{\partial \xi_{\beta_2}}{\partial X_{\alpha}} \int_{\Omega^K} \frac{\partial \Phi_i}{\partial \xi_{\beta_1}} \frac{\partial \Phi_j}{\partial \xi_{\beta_2}} dX \quad (3.7)$$

This can be written as a tensor contraction:

$$M_L^e[i, j] = \sum_{\beta_1=1}^{N_{dim}} \sum_{\beta_2=1}^{N_{dim}} A_{ij\beta} G_K^{\beta} \quad \Rightarrow \quad M^e = A : G_K \quad (3.8)$$

where

$$A_{ij\beta} = \int_{\Omega^K} \frac{\partial \Phi_i}{\partial \xi_{\beta_1}} \frac{\partial \Phi_j}{\partial \xi_{\beta_2}} dX, G_K^{\alpha} = |J^K| \sum_{\alpha=1}^{N_{dim}} \frac{\partial \xi_{\beta_1}}{\partial X_{\alpha}} \frac{\partial \xi_{\beta_2}}{\partial X_{\alpha}} \quad (3.9)$$

This optimisation reduces the number of arithmetic operations required from  $N_q n_0^2 d$  to  $d^3 + N_0^2 d^2 \sim n_0^2 d^2$  where  $N_q$  is the number of quadrature points,  $n_0$  is the polynomial order of the basis, and  $d$  is the number of dimensions. Since the number of dimensions is almost always 2 or 3, the reduction in operations is roughly a factor of  $N_q$ , which can be a significant reduction for high order basis functions.

We remark that although this particular example is specific to the Laplacian form, the key part of this optimisation is the change of variables, which may be applied to any integral form. There are other examples of similar optimisations that may be used in cases when the transform from the reference element to the physical element is not affine, discussed in [Kirby and Logg, 2006] and [Logg, 2007].

It is thought that this transformation is part of a more general class of transformations that reduces the operation count of constructing the global matrix and global vector. These operations are based around rewriting terms under an integral, in order that part of the rewritten term becomes constant over an element. These newly-created constant terms can be moved outside the integral in order to reduce the complexity of the computations that need to be performed for every element.

## 3.6 Related Areas

In this section we examine literature that is not directly related to the finite element method, but from which we can draw ideas that may integrate well with the proposed research. We suggest how these ideas may be relevant to the development of our project.

### 3.6.1 Library Generators

A number of tools for generating optimised libraries for specific domains exist, including Built To Order BLAS [Belter *et al.*, 2009, Jessup *et al.*, 2010] for linear algebra, SPIRAL [Püschel *et al.*, 2005] for DSP transforms, and the Tensor Contraction Engine [Auer *et al.*, 2006]. We discuss SPIRAL and the Tensor Contraction Engine in more detail below in order to discuss concepts that could also be applied to the generation of finite element solvers.

#### SPIRAL

SPIRAL [Püschel *et al.*, 2005] is a platform for generating highly efficient code for DSP transforms. The motivation for its development is the observation that traditional compilers do a poor job of optimising C code for DSP transforms. This is because the C code contains no semantic information regarding the choice of algorithm, so the compiler is forced to make the most general assumptions about the code, inhibiting optimisation.

DSP transforms are defined using the *Signal Processing Language* (SPL), which uses a matrix algebra representation. SPL constructs are manipulated according to a set of rules that allow a complex transform to be rewritten in terms of simpler ones (e.g. the Cooley-Tukey rule), or that perform algebraic rewrites by using matrix identities. These rules may be repeatedly applied to generate a broad class of algorithms that perform the same computation.

The various implementations are converted into an SSA-form [Aho *et al.*, 2006] intermediate representation ( $\Sigma$ -SPL). Standard optimisations including loop unrolling, intrinsic precomputation, common subexpression elimination etc. are applied to this representation. These optimised representations are converted to scalar C code or vector code using intrinsics for the target platform. The choice of vector intrinsics is influenced by a description of the available operations on the target hardware. A similar process is used to generate code for multiprocessor systems and GPUs, although this work is still under development [SPIRAL Project, 2010].

There is a large variation in the performance of the generated implementations of transforms. In order to select the best implementations, learning and search techniques are used. The learning framework is used to prune the search space by removing candidate implementations that are expected to perform poorly, based on automatically built performance models of the operations that constitute each implementation. Dynamic programming [Bellman, 2003] and evolutionary search [Goldberg, 1989] are used to find the best candidates in the remaining space of possible implementations.

We remark that there is almost a direct analogy between SPIRAL and the FEniCS tools. In both projects, high-level domain-specific languages are used as a source from which to generate optimised code. It is conjectured that the techniques used in SPIRAL to generate efficient DSP transforms may be translated to generate efficient implementations of finite element codes on GPUs. In particular, the idea of using a rulebase to guide transformations of an algorithm is applicable to the finite element method, as demonstrated in Section 3.5. The generation of a space of possible implementations of finite element algorithms may also necessitate mechanisms for pruning the search space.

We also note that techniques for searching for the optimal implementation may also be applied at a lower level: there is a space of possible kernel fusions that may be made, and some mechanism for searching this space will be required. Additionally, characteristics of the target hardware such as the L1 cache size, the number of SMs on the device, and the number of registers etc. may form part of a performance model that is used to guide this search.

## The Tensor Contraction Engine

The Tensor Contraction Engine [Auer *et al.*, 2006, Baumgartner *et al.*, 2002] is used for searching for the best implementation of tensor contractions, given restrictions on storage space at various memory hierarchy levels. We consider an example given in [Baumgartner *et al.*, 2002]:

$$S_{abij} = \sum_{cdefkl} A_{acik} \times B_{befl} \times C_{dfjk} \times D_{cdel} \quad (3.10)$$

This expression may be evaluated using ten nested loops in  $4 \times N^{10}$  operations, where the range of each index is  $N$ . The same result can be computed in  $6 \times N^6$  operations by rearranging the expression:

$$S_{abij} = \sum_{ck} \left( \sum_{df} \left( \sum_{ef} B_{befl} \times D_{cdel} \right) \times D_{dfjk} \right) \times A_{acik} \quad (3.11)$$

However, this new expression requires a large amount of temporary storage, which may exceed the memory capacity of the target machine. There are a large set of expressions that perform an equivalent computation to Equations 3.10 and 3.11, requiring various amounts of computation and storage. Manipulation of the tensor expression to produce various different versions is relatively straightforward, especially using a package such as Matlab [MathWorks, 2009]. However,

```

continuous (* Pendulum physics *)
  m = 5.0; g = 9.81; l = 3;
  I = m * l^2;
  F*l*cos(theta) - m*g*l*sin(theta) = I*theta'';

boundary conditions
  theta with theta(0) = 0.1, theta'(0) = 0;

```

Figure 3.5: An Acumen description of the physics of a pendulum. Note that `theta` is an independent variable that changes over time. From [Zhu *et al.*, 2010].

producing an implementation of the computation and benchmarking it requires a relatively large effort to implement the trivial code needed to implement each expression.

In order to overcome this problem, the TCE provides a domain-specific language for writing down a tensor expression. An optimal implementation of the expression that requires a minimal amount of computation given memory and disk space limits is searched for, and an implementation is automatically generated. This greatly reduces the burden on the programmer in implementing tensor contraction operations.

A similar situation arises in the implementation of finite element methods on GPUs. Using a greater number of smaller kernels increases the total number of threads that can run concurrently and increases performance. However, using more kernels requires more intermediate storage arrays. In this case, the use of memory bandwidth rather than memory space becomes an issue, as the performance of the kernels becomes limited by their ability to transfer data to and from global memory. Out of these possible implementations, a search is required to find the optimum kernel granularity subject to the constraints on the occupancy of individual kernels.

### 3.6.2 Acumen

The Acumen system [Zhu *et al.*, 2010] provides the user with a domain-specific language for specifying the ordinary differential equations governing a mechanical system. Figure 3.5 gives a short example of the Acumen source describing a pendulum. The Acumen compiler performs some analysis and transformation on the equations in the source file, in order to transform them into a system that can be stepped forward in time using a Runge-Kutta method.

The system of equations go through several phases of analysis and transformation in order to reach their final form, including a defined variable analysis, binding time analysis, and symbolic differentiation. A key contribution of the Acumen system is the binding time analysis, that is used to provide information to the symbolic differentiation phase that allows it to reduce the complexity of the generated expression. In contrast, tools such as Matlab must make more general assumptions about equations they are differentiating symbolically, leading to the generation of much larger expressions than are required.

Although we do not cover this defined variable analysis in detail, we note that at the heart of this transformation is the concept of using domain-specific knowledge to reduce the complexity of the generated code. The use of similar analyses in the finite element context might be used to reduce the complexity of the code for evaluating multilinear forms, perhaps as part of a system that performs algebraic transformations of the forms.

### 3.6.3 Autotuning Libraries

Self-tuning libraries for particular domains maximise performance on a particular target by performing extensive benchmarking and tuning at installation time. There are examples of these libraries for a number of different domains, including ATLAS [Whaley and Dongarra, 1998, Whalley, 2005] for linear algebra, OSKI [Vuduc *et al.*, 2005, Vuduc, 2003] for sparse matrix operations, and FFTW

[Frigo and Johnson, 2005] for Fourier transforms. The search performed at installation time can be very time-consuming, but only needs to be performed once.

Since the performance characteristics can vary from machine to machine depending on factors such as the number of cores, number of processors, size and latency of each level in the memory hierarchy etc., the use of automatic tuning ensures that the best possible implementation is used on each machine. In relation to implementations of the finite element method, we note that the search space of implementations when considering various algebraic rewrites as well as kernel fusions and other optimisations may become large. In the absence of more sophisticated search techniques, performing brute-force autotuning to generate the best implementation of a solver for a particular UFL source may be an option.

### 3.6.4 Active Libraries

Active Libraries [Czarnecki *et al.*, 2000] perform optimisation of computations by generating specialised implementations, at runtime or at compile time using expression templates. Active libraries include DESOLA for linear algebra [Russell *et al.*, 2008], Blitz++ [Veldhuizen, 1998] and the Matrix Template Library [Siek, 1999] for matrix operations, and Bernoulli for sparse matrix operations [Ahmed *et al.*, 2000].

A feature that these libraries have common is that they are all designed to be used from inside a low-level language, such as C++, rather than as part of a domain-specific language. Since the UFL representation is high-level and retains necessary semantic information about the computations, it is difficult to map the techniques used by active libraries onto code generation of finite element methods using UFL.

### 3.6.5 Formal Linear Algebra Methods Environment

The Formal Linear Algebra Methods Environment (FLAME) [Gunnels *et al.*, 2001, Bientinesi *et al.*, 2005] systematises the development of linear algebra algorithms and their translation into code. In order to derive an algorithm, a *worksheet* is filled in according to conditions on the input and expected output of the algorithm, and also conditions that are required to hold throughout the execution of the algorithm. The completed worksheet specifies the resulting algorithm in an inductive fashion. Although the worksheet must be filled in by hand, there have been some efforts directed towards automatically deriving the filled-in worksheet [Bientinesi, 2006]. The methodology has recently been extended to the derivation of Krylov-subspace solvers [Eijkhout *et al.*, 2010] (examples of Krylov-subspace solvers include the conjugate gradient and GMRES methods).

It is remarked that there is a similarity between the work in [Bientinesi, 2006] on automatically deriving new algorithms, and the techniques used to derive new implementations by making algebraic transformations in SPIRAL, and those described in Section 3.5. The inductive nature of the algorithms produced by worksheet fill-in are substantially different from any of the known algebraic transformations of finite element operations. However, it is possible that formulations of the finite element method in terms of tensor contractions can be treated in this fashion. This could be investigated if it is difficult to find transformation rules of finite element operations in terms of algebraic operations.

## 3.7 Conclusions

We have examined the Unified Form Language from the FEniCS project, which provides a means for declaratively specifying a finite element method. Since the UFL representation is completely independent of the underlying implementation, all of the optimisation techniques that have been examined throughout this chapter may be implemented in a UFL compiler without exposing them to the user. The compilation and optimisation techniques that can be pursued as part of further investigations can be summarised as follows:

**Data layout transformations.** Partitioning and padding techniques that allow more effective use of the memory hierarchy have been described in Sections 3.4 and 3.3.1 respectively.

**Colouring.** Using colouring schemes avoids the need for atomic operations on GPUs, increasing efficiency. The OPlus2 two-level scheme works in conjunction with partitioning, and implementation of this scheme should be investigated.

**Kernel Granularity.** Section 3.3.3 outlined the necessity for choosing the appropriate level of granularity of kernels, and described a scheme for finding an efficient choice of kernel fusions.

**Algebraic Transformations.** In Section 3.5, two examples of algebraic transforms are outlined. It is hypothesised that many algebraic transforms are possible, and that these possible transforms may be enumerated as a set of transformation rules. The implementation space generated by these transformations may be explored using techniques similar to those in SPIRAL and the Tensor Contraction Engine, described in Section 3.6.1.

**Automatic Tuning.** Automated search and tuning techniques (Section 3.6.3) can be used in conjunction with techniques that generate a space of possible implementations, including an algebraic transformation system and a lower level system for generating implementations of different kernel granularities.

Manual investigations of these areas will be time-consuming. In order to reduce the time taken to perform investigations, and to work towards the eventual goal of providing tools that automatically generate efficient GPU implementations of finite element solvers from high-level sources, it is pragmatic to begin by implementing a UFL compiler that generates GPU implementations. This can then be followed by the implementation of these transformations and optimisations in the code generator. The following chapter describes preliminary investigations into some of these areas that have already taken place. Chapter 5 goes on to describe a plan for carrying out this research over the course of the PhD.



# Chapter 4

## Preliminary Investigations

### 4.1 Introduction

In this chapter we describe some experiments that investigate the performance of two algorithms for the global assembly phase on the GPU, and a prototype implementation of a UFL compiler. The content of this chapter has been published as part of [Markall *et al.*, 2010c].

A complete implementation of a test problem has been developed that executes all computations on the GPU, and this is used as the basis for our experiments. We also discuss a data layout transformation that was necessary to obtain coalescing, and therefore make use of a substantial portion of the available memory bandwidth of the device. These experiments show that the optimal algorithm depends on the target hardware.

The implementation of the prototype UFL compiler that generates CUDA code is also described. The performance of the generated code is not investigated, but instead we use the experience gained from this exercise to map out the future work that needs to be done in order to implement a more complete compiler.

### 4.2 Data Format Considerations

In general, data structures must be carefully chosen to achieve optimal performance (e.g. for cache-optimality on a CPU), and the optimal choice of data structure depends on characteristics of the target architecture. In order to examine the structures that can be used when implementing the finite element method on CPUs and GPUs, we consider a three element domain (see Figure 4.1).

In CPU implementations, nodal data is often stored on a per-node basis. When data for the nodes of a single element is needed, the mapping array (map) is used to indirectly access the nodal data. Although this can lead to poor cache performance due to random access into the nodal data structure, reordering optimisations can be used to minimise this overhead.

This data format is inefficient for GPU implementations, where coalesced accesses must be used to maximise memory performance. It is difficult to achieve coalesced access because the

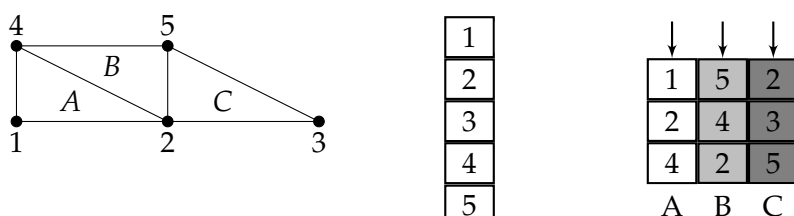


Figure 4.1: *Left:* A 2D domain decomposed into three elements. *Middle:* Node data layout in CPU implementation. *Right:* Node data layout in GPU implementation. Threads accessing data in different elements (arrowed) achieve coalescing.

nodal data structure is accessed in a somewhat random fashion. We propose that it can be more efficient to store nodal data on a per-element basis in GPU implementations, interleaving the nodal data for each node of each element. This leads to some redundancy in the storage of nodal data, again proportional to the average variance of nodes; however, it allows coalesced accesses when there is a one-to-one mapping between threads and elements.

## 4.3 Experiments

We evaluate the performance of the Addto algorithm and the Local Matrix Approach on GPUs using an implementation of a test problem that solves the advection-diffusion equation:

$$\frac{\partial T}{\partial t} + \mathbf{u} \nabla T = \nabla \cdot \bar{\bar{\mu}} \cdot \nabla T$$

where  $T$  is the concentration of a tracer,  $t$  is time,  $\mathbf{u}$  is velocity, and  $\bar{\bar{\mu}}$  is a rank-2 tensor of diffusivity. This problem is chosen as it is both a sub-problem and simplified model of a full computational fluid dynamics system. The system is discretised using order-1 basis functions. A split scheme is used, solving for advection first and then diffusion at each time step. The advection term is timestepped using a 4th-order Runge-Kutta scheme, and the diffusion term is timestepped using an implicit theta scheme. The problem is solved over a square domain with suitable initial conditions. We compare with a CPU implementation to demonstrate that the optimal choice of algorithm depends on the target hardware.

### 4.3.1 CUDA and CPU Implementations and Experimental Setup

CUDA Implementations of the solver that implement both the Addto algorithm and the Local Matrix Approach have been produced. The Local Matrix Approach is implemented by considering the computation in Equation 3.3 in three stages:

$$\underbrace{\mathbf{t} = \mathcal{A}\mathbf{v}}_{\text{Stage 1}}, \quad \underbrace{\mathbf{t}' = \mathbf{M}^e \mathbf{t}}_{\text{Stage 2}}, \quad \underbrace{\mathbf{y} = \mathcal{A}^T \mathbf{t}'}_{\text{Stage 3}}.$$

Since  $\mathcal{A}$  contains only one non-zero entry per row that is always 1, Stage 1 is implemented as a gather. This involves uncoalesced memory accesses but is more efficient than using an SpMV kernel. The implementation of Stage 2 exploits the block-diagonal structure of  $\mathbf{M}^e$  to achieve coalesced accesses and maximal reuse of matrix values. Stages 1 and 2 are implemented in a single kernel. Stage 3 is implemented as an SpMV kernel that is optimised for all the non-zero values equalling 1. Because a global barrier is required between Stages 2 and 3, Stage 3 is implemented in a separate kernel.

The baseline version is implemented within Fluidity because it is a mature and optimised CPU implementation. The Local Matrix Approach is not implemented in this version, as it is known to be less efficient than the Addto algorithm on CPUs for low-order basis functions [Vos *et al.*, 2009]. Node data structures are implemented using the element-wise storage layout in the CUDA implementation, and the node-wise layout is used in the CPU implementation.

The test hardware consists of an Intel Core 2 Duo E8400, 2GiB RAM, and an NVidia 280GTX GPU. The Intel v10.1 compilers with the `-O3` flag were used for the CPU code (v11.0 onwards cannot compile Fluidity due to compiler bugs), and the CUDA SDK 2.2 is used for CUDA code. The CUDA implementation uses a *Conjugate Gradient* (CG) solver described in [Markall and Kelly, 2009]; the baseline version make use of the PETSc [Balay *et al.*, 2009] CG solver. The simulation is run for 200 timesteps, with all computations using double precision arithmetic. Gmsh [Geuzaine and Remacle, 2009] was used to generate meshes varying in size between 28710 and 331714 elements. Each simulation was run five times, and averages are reported.

### 4.3.2 Results

Figure 4.2 shows the total time taken by each CUDA implementation to run the entire simulation. Figure 4.3 shows their speedup relative to the baseline version running on 2 cores. We see that the LMA implementation is up to 2.2 times faster than the Addto implementation on the GPU, and is over an order of magnitude faster than the baseline implementation.

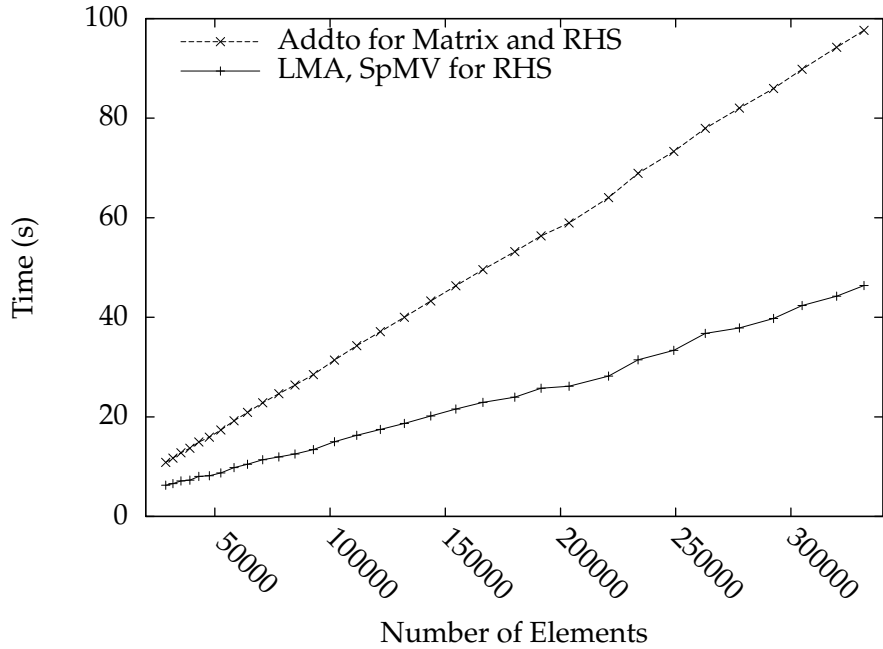


Figure 4.2: Total execution time of GPU implementations.

Figure 4.4 shows the total time taken for the local and global assembly phases in the CUDA implementations. We observe that the Local Matrix Approach is faster than the Matrix Addto algorithm, and that it is faster to assemble the global vector by computing the product  $\mathcal{A}^T \mathbf{b}^e$ . Figure 4.1 shows the total time spent inside the SpMV kernels for each implementation for the largest and smallest mesh sizes. The cost of computing  $(\mathcal{A}^T (\mathbf{M}^e (\mathcal{A} \mathbf{v})))$  (in the LMA implementation) is up to 2.5 times that of computing  $\mathbf{Mv}$  (in the Addto implementation). The performance increase of the LMA implementation is a tradeoff between the decrease in the assembly time, and the increase in the SpMV computation time.

Elements	$(\mathcal{A}^T (\mathbf{M}^e (\mathcal{A} \mathbf{v})))$	$\mathbf{Mv}$
28710	$1.91 \times 10^6$	$8.48 \times 10^5$
331714	$2.45 \times 10^7$	$9.85 \times 10^6$

Table 4.1: Total time spent computing each product on the largest and smallest meshes (in  $\mu$ sec), recorded using the CUDA Profiler.

We also investigated using graph colouring to eliminate atomic operations in the Addto implementation (as used in [Komatitsch *et al.*, 2009]). We replaced atomic operations with equivalent non-atomic operations. The resulting implementation produced incorrect results, but gave an upper bound on the performance increase facilitated by colouring. The assembly phase ran 25% faster with non-atomic operations, corresponding to a 10% speedup in the entire simulation. Since the performance of the LMA implementation is far greater than this, it is unnecessary to produce an implementation that uses colouring.

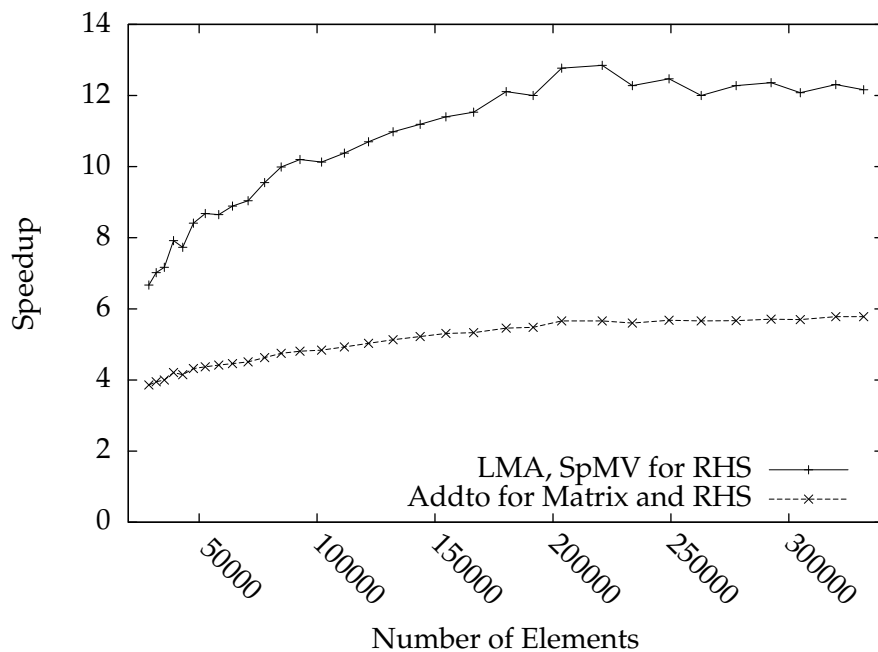


Figure 4.3: Speedup of GPU implementations relative to the baseline executing using 2 cores.

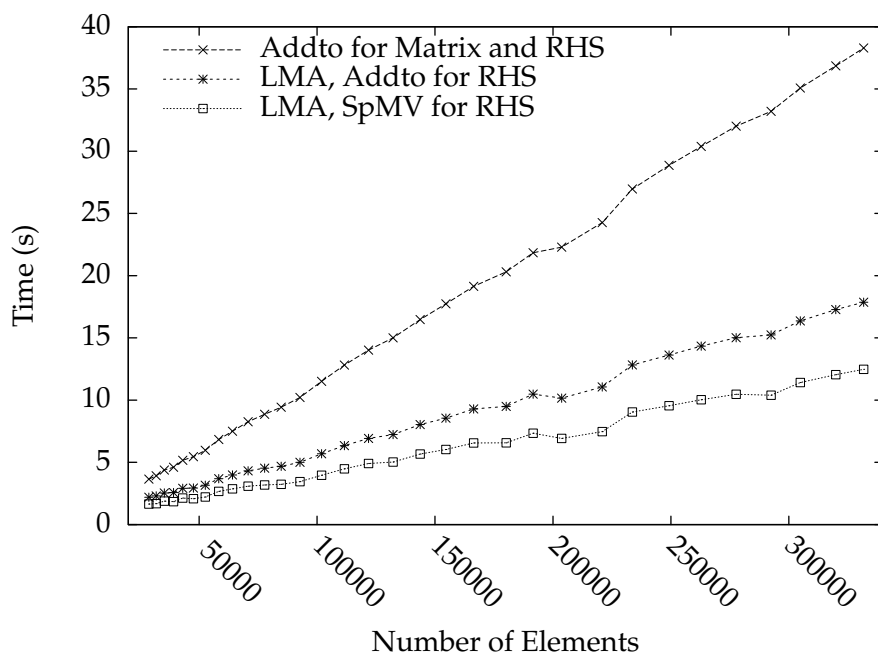


Figure 4.4: Execution time of the assembly phases for each CUDA implementation.

## 4.4 Further Investigations

Our results show that the optimal algorithm depends on the target architecture. We speculate that it is also problem-dependent. In a 2D domain the average variance of nodes is approximately 6. In a 3D domain, the variance is around 24, and the overheads of storage and computation for the local matrix approach are four times greater than in 2D. This extra overhead may decrease performance to the point where it is more efficient to use the Addto algorithm. Our further work involves investigating the performance in this case.

## 4.5 A Prototype Compiler

A first step in experimenting with generating CUDA code from UFL involved the implementation of a compiler that performs a syntax-directed translation of the UFL code to CUDA code. The generated code uses a library of kernels that perform common operations in finite element assembly. A subset of the kernels in this library are shown in Table 4.2. These kernels perform quadrature-based assembly, rather than the tensor-based method that is used in the FEniCS project.

The compiler inputs UFL using the FEniCS UFL distribution [Alnæs and Logg, 2009] to produce *Directed Acyclic Graphs* (DAGs) of the operations specified in a UFL source. Each DAG node is converted to a call to a kernel implementing the required operation. This DAG of kernel calls is passed to a code generator that is implemented using the ROSE Compiler Infrastructure [Quinlan *et al.*, 2009]. Examples of the DAGs for the left-hand side of Equation 3.2 are shown in Figure 4.5.

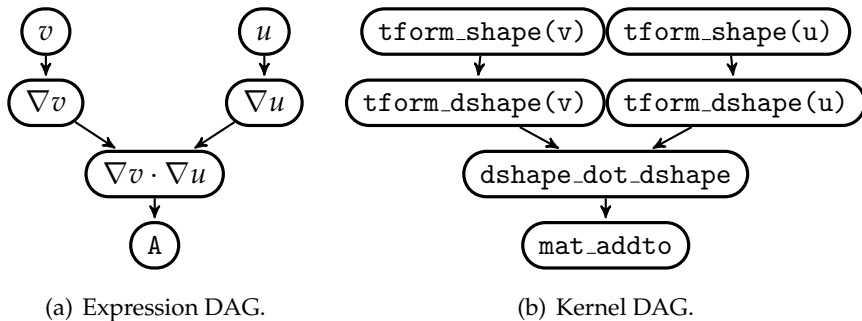


Figure 4.5: DAGs for the form  $\int_{\Omega} \nabla v \cdot \nabla u \, dX$ .

Kernel	Operation
tform_shape	Transform basis functions from reference space to physical space.
tform_dshape	Transform derivatives of basis functions to physical space.
dshape_dot_dshape	Computes $\int_{\Omega} \nabla v \cdot \nabla u \, dX$ .
shape_shape	Computes $\int_{\Omega} vu \, dX$ .
mat_addto	Adds local matrices into a global matrix using the Addto algorithm.

Table 4.2: A subset of kernels in the CUDA kernel library.

The CUDA code generated by this compiler for the Poisson problem produces identical results to a handwritten CUDA implementation, as well as a CPU implementation of the same problem. Although the generated code executes faster than the CPU implementation for large meshes, we do not investigate its performance as there is only a limited speed improvement that can be gained for steady-state problems.

### 4.5.1 Further UFL Compiler Development

Although the prototype compiler demonstrates the feasibility of generating CUDA code from UFL sources, the requirement for a library of handwritten CUDA kernels limits its output to a

pre-defined set of forms optimised by hand. Here we describe an intermediate phase that lowers the UFL representation to one amenable to optimisation with established techniques before being used to generate CUDA kernels. Consider one term from the weak form of the Helmholtz equation [Karniadakis and Sherwin, 1999]:

$$\int_{\Omega} \nabla v \cdot \nabla u + \lambda v u \, dX \quad (4.1)$$

There are several combinations of kernels that implement the local assembly phase of this term that can be implemented. We can enumerate these possibilities by building an *Intermediate Representation* (IR) that provides a high-level semantic representation of each term. Sub-terms of the intermediate representation are determined by working bottom-up from leaf nodes to identify the smallest set of nodes that describes the assembly of a local matrix. Higher sub-terms are identified as the addition or scalar multiplication of lower-sub terms.

The IR for Equation 4.1 is shown in Figure 4.6. As there are four sub-terms, up to four separate kernels may perform local assembly for this term. Using more kernels increases the memory bandwidth requirements; however, larger kernels require more resources, decreasing the total parallelism [Filipovic *et al.*, 2009a]. Instead of building a performance model to evaluate each candidate implementation, a pragmatic approach is to lower this representation to one that can be optimised using existing techniques.

Each of the nodes at the root of the sub-terms may be lowered to a loop over a certain index. For example, the `sum` node corresponds to a loop over the elements that sums the local matrices produced by the lower sub-terms. The generated loop nest can be optimised using standard techniques, for example in the polyhedral model [Pouchet *et al.*, 2007] or the *Æcute* framework [Howes *et al.*, 2009].

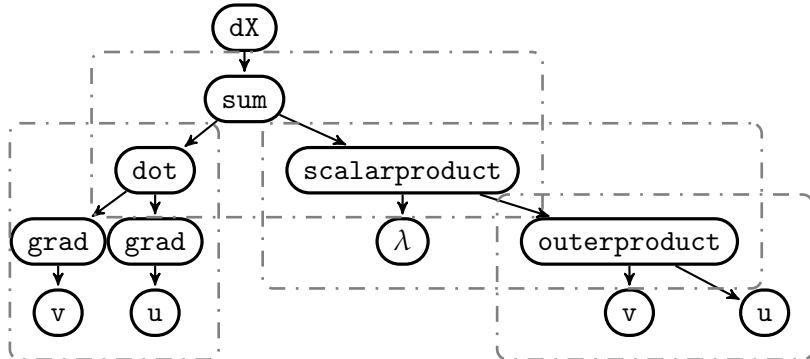


Figure 4.6: Intermediate Representation of the term  $\int_{\Omega} \nabla v \cdot \nabla u + \lambda v u \, dX$ . Sub-terms are indicated by dotted outlines.

## 4.6 Conclusions

The experimental results that have been presented have shown that the Local Matrix Approach gives superior performance compared to the Addto algorithm when implementing the finite element method on a GPU in 2D using order-1 basis functions. We have also seen that changes in the data format and the structure of the assembly loop are necessary. All of these changes are represented by the same UFL source code, and a compiler is free to make choices about each of these aspects.

We have also discussed the implementation of a prototype UFL compiler that generates code reliant on a library of hand-written local matrix assembly kernels. Since we have found that this is not an efficient approach, current work is based upon reimplementing this compiler so that it generates kernels based on specific forms that are in the UFL source. A suitable intermediate representation has been outlined. It is expected that this representation will allow the generation

of different implementations that have been produced using polyhedral transformations, or other optimisations. The work on this compiler and the results that are expected to be produced are outlined in the following chapter.



# Chapter 5

## Research Plan

### 5.1 Introduction

This chapter maps out the work that needs to be done before the completion of the PhD. The work can be broken into several distinct chunks, some of which are independent. Figure 5.1 shows how these tasks are broken down and the periods in which they will be completed. It is expected that publications should result from the work that is completed. Several possible publications are mapped out on the timeline. It is not expected that each of these potential publications will develop into a full submission - it is possible that some will be amalgamated, depending on the value of the contribution that is derived from the work on which the publications are based.

### 5.2 Work Items

**1 - MCFC Development.** The work towards producing a form compiler that inputs UFL sources and generates CUDA code that integrates with Fluidity is to be completed. This compiler is referred to as the *ManyCore Form Compiler*, or MCFC. In order to complete this, a code generator that produces CUDA kernels that compute individual forms from a UFL source must be produced. A second portion of the compiler will generate code that calls these kernels in the correct order with the correct parameters, and handles flow control (for example, for timestepping). A final portion of the code generation will produce code that extracts the required data from Fluidity's data structures and marshals it onto the GPU.

UFL code that solves Poisson's Equation and an advection-diffusion problem will be generated first, to aid in debugging. An implementation of a shallow-water equations [Wesseling, 2001] solver will then be produced, and its output validated by comparing it to the output of a shallow-water solver that is part of Fluidity.

**2 - MCFC Performance Optimisations.** Potential performance optimisations that are identified in the literature review are to be implemented. These include:

- Generating kernels that contain a number of fused operations. This idea is based on the decomposition-fusion scheme identified in Section 3.3.3.
- Adding code that loads small partitions of the mesh into shared memory to local matrix assembly kernels.
- Further algebraic transformations may be incorporated, such as the evaluation by tensor representation described in Section 3.5.2.

**3 - OpenCL Investigation.** Following the work of a UROP student over the summer of 2010, an MCFC backend that generates OpenCL code instead of CUDA code will be developed. This will allow the generated code to be run on most multicore and manycore architectures. Since the performance characteristics of these architectures are very different, this will allow further experimentation to find the choices of optimisations/transformations that best suit a particular target architecture.

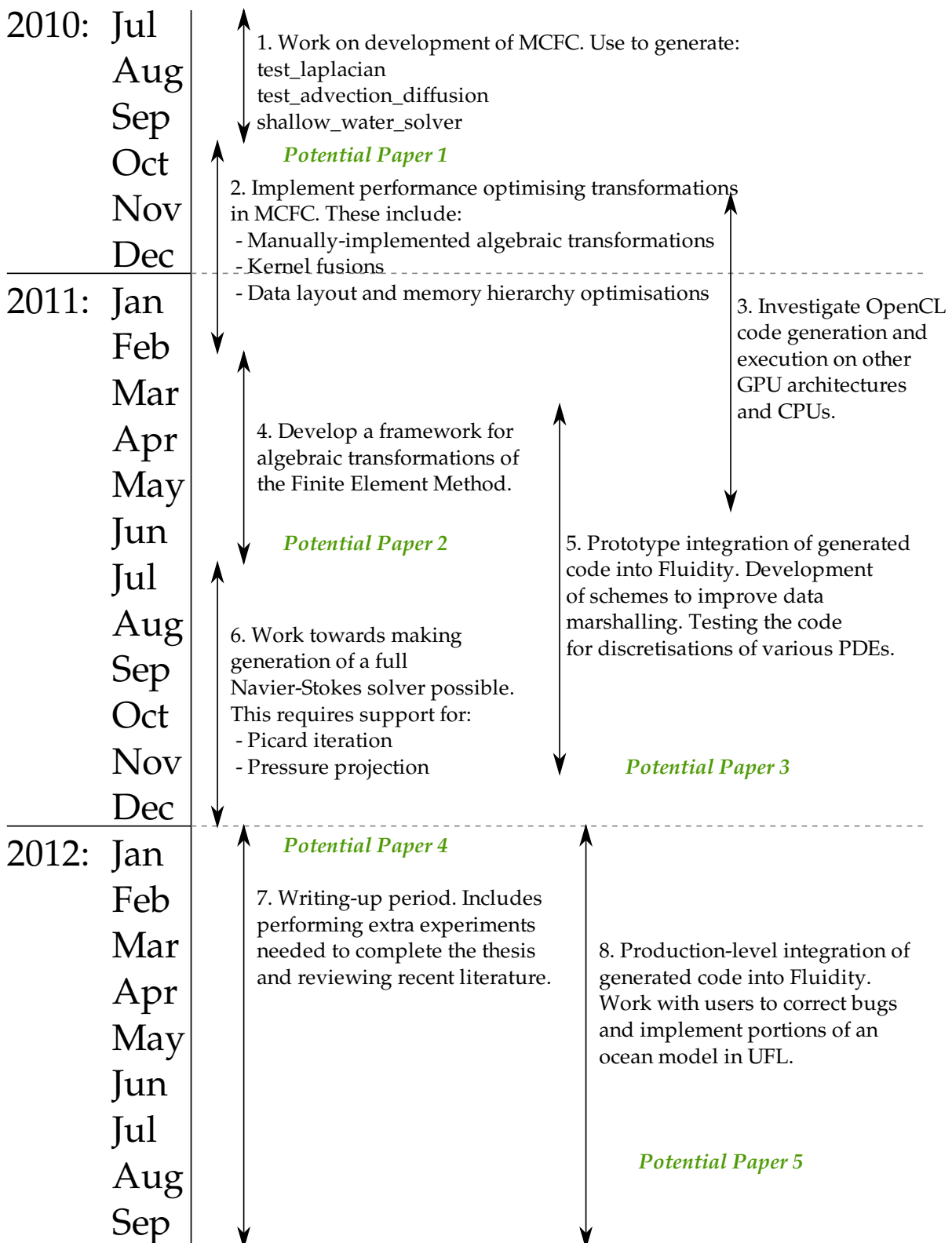


Figure 5.1: Timeline showing tasks until the completion of the PhD.

**4 - Algebraic Transformations.** Similarly to the SPIRAL project, it is expected that the Finite Element Method may be represented as a set of algebraic operations that may be transformed by a set of rules, to generate a whole space of possible implementations. It is expected that the optimal choice of transformations is different for each architecture, and it is hoped that it is possible to develop methods to guide the transformations with a knowledge of the target architecture.

**5 - Fluidity Integration.** Since one of the main goals of this project is to provide tools for automatically generating code to the users/developers of Fluidity, it is necessary to consider how the generated code integrates into Fluidity on a large scale. This work unit will involve experimenting with integrating generated code into the main Fluidity codebase. Due to the size of Fluidity and the various non-finite element operations that it performs (such as mesh adaptivity). It is expected that issues will arise in managing data placement and ensuring that data freshness is maintained across different architectures. Accordingly, a large proportion of time has been set aside to overcome these issues whilst still maintaining performance.

**6 - Navier Stokes.** Since the motion of fluids is generally described by the Navier-Stokes equations [Wesseling, 2001], and form a large part of the numerical computations in Fluidity, it is important to work towards the generation of a solver for these equations from UFL sources. In order to achieve this, MCFC must be extended to generate code for Picard iteration, in order to compute the nonlinear term.

**7 - Writing Up.** The thesis will be finalised at this stage. Further experiments that are required to complete the research may also be run at this stage.

**8 - Fluidity Deployment.** The tools for generating code will be passed on to the developers of Fluidity, and used to integrate generated code that assembles a large portion of the systems that are solved in Fluidity. This will include the implementation of terms such as gravity, buoyancy, surface tension, viscous, coriolis geostrophic pressure etc. It is hoped that there will be two-way communication with developers, leading to improvements in MCFC as well as bugfixes and usability improvements. The experiences from this work item will also be integrated into the thesis in Work Item 7.

### 5.3 Potential Publications

1. This publication is based upon the work completed in Work Item 1. The expected contribution includes a description of the implementation of MCFC. This is novel since there are currently no compilers for UFL that generate CUDA code, and because the issues arising from the implementation are non-trivial. It is expected that some code-generation choices will be embedded into MCFC, including the choice of either the Local Matrix Approach or the Addto algorithm. Performance results for each of the implementations may be compared in the publication.
2. This publication is based upon the work in Work Items 2 and 4, and possibly 3. The contribution will be the presentation of the algorithms for performing algebraic transformations on finite element implementations, and a discussion of the rules contained within the rulebase. Performance results for various architectures that demonstrate how the choice of transformations affects the performance will be presented.
3. This publication is based upon the Work Item 5. The contribution will be based around the work needed to integrate generated code into Fluidity, in particular the techniques required to maintain consistency of data across different nodes and architectures, whilst maintaining performance by transferring data efficiently.
4. This publication is based on Work Item 6, and will discuss the implementation and performance of the Navier-Stokes solver on CPU and GPU architectures. It is expected that part

of the contribution will describe the efficient implementation of boundary conditions on manycore architectures.

5. This publication is based on all the Work Items, and is expected to be an article summarising the state of the research, and in particular drawing attention to the large-scale models that are able to be simulated with generated code, as well as the improvement in software development that is brought about by the use of a high-level language for development.
6. Another publication that can be developed relatively independently of the other work in the timeline involves determining the grammar for UFL, and assigning a semantics and type system to the constructs generated by this grammar. This will provide a contribution to the community, since there is presently no formal definition of UFL.

## 5.4 Conclusions

The research that has been completed so far has laid the foundations for the development of tools for generating high-performance finite elements solvers on manycore architectures. The eventual goal of this research is to provide these tools to users that will benefit from them, both in terms of ease of development and the performance of the resulting code.

The long-term goal (beyond the scope of this PhD) is to rewrite a large portion of Fluidity using UFL. The result of this work will be a portable and maintainable high-performance code that allows aggressive exploitation of future architectures.

# Bibliography

[Ahmed *et al.*, 2000] Nawaaz Ahmed, Nikolay Mateev, and Keshav Pingali. A framework for sparse matrix code synthesis from high-level specifications. In *Supercomputing '00: Proceedings of the 2000 ACM/IEEE conference on Supercomputing (CDROM)*, page 58, Washington, DC, USA, 2000. IEEE Computer Society.

[Aho *et al.*, 2006] Alfred V. Aho, Monica S. Lam, Ravi Sethi, and Jeffrey D. Ullman. *Compilers: Principles, Techniques, and Tools (2nd Edition)*. Addison Wesley, August 2006.

[Alnæs and Logg, 2009] Martin Alnæs and Anders Logg. UFL Specification and User Manual 0.1. URL: <http://www.fenics.org/pub/documents/ufl/ufl-user-manual/ufl-user-manual.pdf>, April 2009.

[AMD, 2010] AMD. AMD: Unleashing the power of parallel compute. [http://sa09.idav.ucdavis.edu/docs/SA09\\_AMD\\_IHV.pdf](http://sa09.idav.ucdavis.edu/docs/SA09_AMD_IHV.pdf), retrieved 10 June 2010, 2010.

[Auer *et al.*, 2006] A.A. Auer, G. Baumgartner, D.E. Bernholdt, A. Bibireata, V. Choppella, D. Cociorva, X. Gao, R. Harrison, S. Krishnamoorthy, S. Krishnan, et al. Automatic code generation for many-body electronic structure methods: the tensor contraction engine. *Molecular Physics*, 104(2):211–228, 2006.

[Bagheri and Scott, 2004] Babak Bagheri and L. Ridgway Scott. About Analysa. Technical Report TR-2004-09, University of Chicago, 2004.

[Balay *et al.*, 2009] Satish Balay, Kris Buschelman, William D. Gropp, Dinesh Kaushik, Matthew G. Knepley, Lois Curfman McInnes, Barry F. Smith, and Hong Zhang. PETSc Web page, 2009. <http://www.mcs.anl.gov/petsc>.

[Bangerth *et al.*, 2007] W. Bangerth, R. Hartmann, and G. Kanschat. *deal. II A general-purpose object-oriented finite element library*. ACM New York, NY, USA, 2007.

[Baumgartner *et al.*, 2002] G. Baumgartner, D.E. Bernholdt, D. Cociorva, R. Harrison, S. Hirata, C.C. Lam, M. Nooijen, R. Pitzer, J. Ramanujam, and P. Sadayappan. A high-level approach to synthesis of high-performance codes for quantum chemistry. In *Proceedings of the 2002 ACM/IEEE conference on Supercomputing*, pages 1–10. IEEE Computer Society Press Los Alamitos, CA, USA, 2002.

[Bellman, 2003] Richard Bellman. *Dynamic Programming*. Dover Publishing, 2003.

[Belter *et al.*, 2009] Geoffrey Belter, E. R. Jessup, Ian Karlin, and Jeremy G. Siek. Automating the generation of composed linear algebra kernels. In *SC '09: Proceedings of the Conference on High Performance Computing Networking, Storage and Analysis*, pages 1–12, New York, NY, USA, 2009. ACM.

[Bientinesi *et al.*, 2005] Paolo Bientinesi, John A. Gunnels, Margaret E. Myers, Enrique S. Quintana-Ortí, and Robert A. van de Geijn. The science of deriving dense linear algebra algorithms. *ACM Transactions on Mathematical Software*, 31(1):1–26, March 2005.

[Bientinesi, 2006] Paolo Bientinesi. *Mechanical Derivation and Systematic Analysis of Correct Linear Algebra Algorithms*. PhD thesis, The University of Texas at Austin, Department of Computer Sciences, August 2006.

[Bordas *et al.*, 2007] Stephane Bordas, Phu Vinh Nguyen, Cyrille Dunant, Amor Guidoum, and Hung Nguyen-Dang. An extended finite element library. *International Journal for Numerical Methods in Engineering*, 71(6):703–732, 2007.

[Brezzi *et al.*, 1985] F. Brezzi, J. Douglas, and LD Marini. Two families of mixed finite elements for second order elliptic problems. *Numerische Mathematik*, 47(2):217–235, 1985.

[Brezzi *et al.*, 1987] F. Brezzi, J. Douglas, M. Fortin, and L.D. Marini. Efficient rectangular mixed finite elements in two and three space variables. *RAIRO - Analyse Numerique - Numer. Anal.*, 21(4):581–604, 1987.

[Cantwell *et al.*, 2010] C.D. Cantwell, S.J. Sherwin, R.M. Kirby, and P.H.J. Kelly. From h to p efficiently: strategy selection for operator evaluation on hexahedral and tetrahedral elements. *Computers and Fluids (submitted)*, 2010.

[Comas *et al.*, 2008] Olivier Comas, Zeike A. Taylor, Jérémie Allard, Sébastien Ourselin, Stéphane Cotin, and Josh Passenger. Efficient Nonlinear FEM for Soft Tissue Modelling and Its GPU Implementation within the Open Source Framework SOFA. In *ISBMS '08: Proceedings of the 4th international symposium on Biomedical Simulation*, pages 28–39, Berlin, Heidelberg, 2008. Springer-Verlag.

[Crouzeix and Raviart, 1973] M. Crouzeix and P.A. Raviart. Conforming and nonconforming finite element methods for solving the stationary stokes equations. *RAIRO - Analyse Numerique - Numer. Anal.*, 7:33–76, 1973.

[Cuthill and McKee, 1969] E. Cuthill and J. McKee. Reducing the bandwidth of sparse symmetric matrices. In *ACM '69: Proceedings of the 1969 24th national conference*, pages 157–172, New York, NY, USA, 1969. ACM.

[Czarnecki *et al.*, 2000] Krzysztof Czarnecki, Ulrich W. Eisenecker, Robert Glück, David Vandervoorde, and Todd L. Veldhuizen. Generative programming and active libraries. In *Selected Papers from the International Seminar on Generic Programming*, pages 25–39, London, UK, 2000. Springer-Verlag.

[Dular and Geuzaine, 2005] P. Dular and C. Geuzaine. *GetDP Reference Manual*, 2005.

[Eijkhout *et al.*, 2010] Victor Eijkhout, Paolo Bientinesi, and Robert van de Geijn. Towards mechanical derivation of krylov solver libraries. *Procedia Computer Science*, 1(1):1799 – 1807, 2010. ICCS 2010.

[Filipovic *et al.*, 2009a] Jiri Filipovic, Igor Peterlik, and Jan Fousek. GPU Acceleration of Equations Assembly in Finite Elements Method - Preliminary Results. In *SAAHPC : Symposium on Application Accelerators in HPC*, July 2009.

[Filipovic *et al.*, 2009b] Jiri Filipovic, Igor Peterlik, and Jan Fousek. GPU Acceleration of Equations Assembly in Finite Elements Method - Preliminary Results. In *SAAHPC : Symposium on Application Accelerators in HPC - Poster Session*, July 2009.

[Filipovic *et al.*, 2010] Jiri Filipovic, Jan Fousek, Ludek Matyska, and Igor Peterlik. Decomposition-Fusion Scheme for Medium-Grained Problems on GPU. Unpublished manuscript, 2010.

[Frigo and Johnson, 2005] Matteo Frigo and Steven G. Johnson. The design and implementation of FFTW3. *Proceedings of the IEEE*, 93(2):216–231, 2005. Special issue on “Program Generation, Optimization, and Platform Adaptation”.

[Geuzaine and Remacle, 2009] Christophe Geuzaine and Jean-François Remacle. Gmsh: A 3-D finite element mesh generator with built-in pre- and post-processing facilities. *Int. J. Numerical Methods in Engineering*, 79(11):1309–1331, 2009.

[Giles, 2010] Mike Giles. A framework for parallel unstructured grid applications on GPUs. Plenary talk at the SIAM conference on parallel processing for scientific computing (PP10), Seattle., February 2010.

[Göddeke *et al.*, 2005] D. Göddeke, R. Strzodka, and S. Turek. Accelerating double precision FEM simulations with GPUs. In F. Hülsemann, M. Kowarschik, and U. Rüde, editors, *18th Symposium Simulationstechnique, Frontiers in Simulation*, pages 139–144. SCS Publishing House e.V., 2005. ASIM 2005.

[Göddeke *et al.*, 2009] Dominik Göddeke, Hilmar Wobker, Robert Strzodka, Jamaludin Mohd-Yusof, Patrick S. McCormick, and Stefan Turek. Co-processor acceleration of an unmodified parallel solid mechanics code with FEASTGPU. *International Journal of Computational Science and Engineering*, 4(4):254–269, October 2009.

[Goldberg, 1989] D.E. Goldberg. *Genetic Algorithms in Search, Optimization and Machine Learning*. Addison-Wesley, Reading, MA, 1989.

[Gorman *et al.*, 2009] Gerard Gorman, Matthew Piggott, and Patrick Farrell. About Fluidity. URL: <http://amcg.ese.ic.ac.uk/index.php?title=FLUIDITY>, November 2009.

[Gschwind *et al.*, 2006] Michael Gschwind, H. Peter Hofstee, Brian Flachs, Martin Hopkins, Yukio Watanabe, and Takeshi Yamazaki. Synergistic Processing in Cell’s Multicore Architecture. *IEEE Micro*, 26(2):10–24, 2006.

[Gunnels *et al.*, 2001] John A. Gunnels, Fred G. Gustavson, Greg M. Henry, and Robert A. van de Geijn. FLAME: Formal Linear Algebra Methods Environment. *ACM Transactions on Mathematical Software*, 27(4):422–455, December 2001.

[Hecht *et al.*, 2005] F. Hecht, O. Pironneau, A. L. Hyaric, and K. Ohtsuka. *FreeFEM++ Manual*, 2005.

[Howes *et al.*, 2009] Lee W. Howes, Anton Lokhmotov, Alastair F. Donaldson, and Paul H.J. Kelly. Deriving efficient data movement from decoupled access/execute specifications. In *Proceedings of the 4th International Conference on High Performance and Embedded Architectures and Compilers (HiPEAC)*, volume 5409 of *Lecture Notes in Computer Science*, pages 168–182. Springer, 2009.

[Jessup *et al.*, 2010] Elizabeth R. Jessup, Ian Karlin, Erik Silksen, Geoffrey Belter, and Jeremy Siek. Understanding memory effects in the automated generation of optimized matrix algebra kernels. *Procedia Computer Science*, 1(1):1867 – 1875, 2010. ICCS 2010.

[Karniadakis and Sherwin, 1999] George E. M. Karniadakis and Spencer J. Sherwin. *Spectral/hp Element Methods for CFD*. Oxford University Press, 1999.

[Karypis and Kumar, 1998] George Karypis and Vipin Kumar. A fast and high quality multilevel scheme for partitioning irregular graphs. *SIAM Journal on Scientific Computing*, 20(1):359–392, 1998.

[Kay, 1988] David C. Kay. *Tensor Calculus*. Schaum’s Outlines. McGraw-Hill, 1988.

[Khronos Group, 2008] The Khronos Group. *OpenCL 1.0 Working Specification*, 2008.

[Kirby and Logg, 2006] R. C. Kirby and A. Logg. A compiler for variational forms. *ACM Transactions on Mathematical Software*, 32(3):417–444, 2006.

[Klöckner *et al.*, 2009] A. Klöckner, T. Warburton, J. Bridge, and J.S. Hesthaven. Nodal discontinuous Galerkin methods on graphics processors. *Journal of Computational Physics*, In Press:–, 2009.

[Klöckner, 2010] Andreas Klöckner. *High-Performance High-Order Simulation of Wave and Plasma Phenomena*. PhD thesis, Brown University, May 2010.

[Komatitsch *et al.*, 2009] Dimitri Komatitsch, David Michéa, and Gordon Erlebacher. Porting a high-order finite-element earthquake modeling application to NVIDIA graphics cards using CUDA. *J. Parallel Distrib. Comput.*, 69(5):451–460, 2009.

[Komatitsch *et al.*, 2010] Dimitri Komatitsch, Dominik Göddeke, Gordon Erlebacher, and David Michéa. Modeling the propagation of elastic waves using spectral elements on a cluster of 192 GPUs. *Computer Science Research and Development*, 25(1-2):75–82, 2010.

[Langtangen, 2003] Hans Petter Langtangen. *Computational Partial Differential Equations, Numerical Methods and Diffpack Programming*. Springer-Verlag, 2003.

[Lipschutz and Lipson, 1997] Seymour Lipschutz and Marc Lipson. *Discrete Mathematics*. Schaum’s Outlines. McGraw-Hill, 2nd edition, 1997.

[Logg and Wells, 2010] Anders Logg and Garth N. Wells. Dolfin: Automated finite element computing. *ACM Trans. Math. Softw.*, 37(2):1–28, 2010.

[Logg, 2007] A. Logg. Automating the finite element method. *Arch. Comput. Methods Eng.*, 14(2):93–138, 2007.

[Long, 2003] K.R. Long. Sundance rapid prototyping tool for parallel PDE optimization. *Large-scale PDE-constrained optimization*, page 331, 2003.

[Maciol *et al.*, 2010] Paweł Maciol, Przemysław Plaszewski, and Krzysztof Banas. 3d finite element numerical integration on gpus. *Procedia Computer Science*, 1(1):1087 – 1094, 2010. ICCS 2010.

[Markall and Kelly, 2009] Graham Markall and Paul H. J. Kelly. Accelerating Unstructured Mesh Computational Fluid Dynamics Using the NVidia Tesla GPU Architecture. ISO Report, Imperial College London, 2009.

[Markall *et al.*, 2009] Graham R. Markall, David A. Ham, and Paul H.J. Kelly. Experiments in unstructured mesh finite element CFD using CUDA. 1st UK CUDA Developers Conference, Oxford, [http://www.industrialmath.net/CUDA09\\_talks/markall.pdf](http://www.industrialmath.net/CUDA09_talks/markall.pdf), Dec 2009.

[Markall *et al.*, 2010a] Graham R. Markall, David A. Ham, and Paul H.J. Kelly. Experiments in generating and integrating GPU-accelerated finite element solvers using the Unified Form Language. FEniCS ’10 Conference, Stockholm, May 2010.

[Markall *et al.*, 2010b] Graham R. Markall, David A. Ham, and Paul H.J. Kelly. Generating optimised multiplatform finite element solvers from high-level representations. 8th IFIP WG 2.11 Working Group on Program Generation, [http://resource-aware.org/twiki/pub/WG211/M8Schedule/Markall\\_M8\\_slides.pdf](http://resource-aware.org/twiki/pub/WG211/M8Schedule/Markall_M8_slides.pdf), Mar 2010.

[Markall *et al.*, 2010c] Graham R. Markall, David A. Ham, and Paul H.J. Kelly. Towards generating optimised finite element solvers for gpus from high-level specifications. *Procedia Computer Science*, 1(1):1809 – 1817, 2010. ICCS 2010.

[MathWorks, 2009] The MathWorks. MATLAB documentation. <http://www.mathworks.com/access/helpdesk/help/techdoc/matlab.html>, Retrieved 17 Oct 2009, 2009.

[Miller *et al.*, 2007] Karol Miller, Grand Joldes, Dane Lance, and Adam Wittek. Total Lagrangian explicit dynamics finite element algorithm for computing soft tissue deformation. *Communications in Numerical Methods and Engineering*, 23(2):121–134, 2007.

[Möes *et al.*, 1999] Nicolas Möes, John Dolbow, and Ted Belytschenko. A finite element method for crack growth without remeshing. *International Journal for Numerical Methods in Engineering*, 46(1):131–150, September 1999.

[Nedelec, 1980] JC Nedelec. Mixed finite elements in R3. *Numerische Mathematik*, 35(3):315–341, 1980.

[NVidia, 2009a] NVidia. NVidia CUDA Programming Guide Version 2.3.1. URL: [http://developer.download.nvidia.com/compute/cuda/2\\_3/toolkit/docs/NVIDIA\\_CUDA\\_Programming\\_Guide\\_2.3.pdf](http://developer.download.nvidia.com/compute/cuda/2_3/toolkit/docs/NVIDIA_CUDA_Programming_Guide_2.3.pdf), August 2009.

[NVidia, 2009b] NVidia. NVIDIA’s Next Generation CUDA Compute Architecture: Fermi. White paper, NVIDIA, 2009. From [http://www.nvidia.com/content/PDF/fermi\\_white\\_papers/NVIDIA\\_Fermi\\_Compute\\_Architecture\\_Whitepaper.pdf](http://www.nvidia.com/content/PDF/fermi_white_papers/NVIDIA_Fermi_Compute_Architecture_Whitepaper.pdf), Retrieved 24 May 2010.

[NVidia, 2010] NVidia. Cuda visual profiler user guide. [http://developer.download.nvidia.com/compute/cuda/3\\_0/toolkit/docs/visual\\_profiler\\_cuda/cudaprof.html](http://developer.download.nvidia.com/compute/cuda/3_0/toolkit/docs/visual_profiler_cuda/cudaprof.html), Retrieved 12 Jun 2010, 2010.

[Piggott *et al.*, 2009] MD Piggott, PE Farrell, CR Wilson, GJ Gorman, and CC Pain. Anisotropic mesh adaptivity for multi-scale ocean modelling. *Philosophical Transactions of the Royal Society A: Mathematical, Physical and Engineering Sciences*, 367(1907):4591, 2009.

[Pouchet *et al.*, 2007] Louis-Noel Pouchet, Cedric Bastoul, Albert Cohen, and Nicolas Vasilache. Iterative optimization in the polyhedral model: Part i, one-dimensional time. In *CGO ’07: Proceedings of the International Symposium on Code Generation and Optimization*, pages 144–156, Washington, DC, USA, 2007. IEEE Computer Society.

[Püschel *et al.*, 2005] Markus Püschel, José M. F. Moura, Jeremy Johnson, David Padua, Manuela Veloso, Bryan Singer, Jianxin Xiong, Franz Franchetti, Aca Gacic, Yevgen Voronenko, Kang Chen, Robert W. Johnson, and Nicholas Rizzolo. SPIRAL: Code generation for DSP transforms. *Proceedings of the IEEE, special issue on “Program Generation, Optimization, and Adaptation”*, 93(2):232–275, 2005.

[Quinlan *et al.*, 2009] Dan Quinlan, Chunhua Liao, Thomas Panas, Robb Matzke, Markus Schordan, Rich Vuduc, and Qing Yi. ROSE: A Tool For Building Source-to-Source Translators. User Manual (version 0.9.4a). [http://www.rosecompiler.org/ROSE\\_UserManual/ROSE-UserManual.pdf](http://www.rosecompiler.org/ROSE_UserManual/ROSE-UserManual.pdf), Retrieved 15 September 2009, 2009.

[Raviart and Thomas, 1977] PA Raviart and JM Thomas. Primal hybrid finite element methods for 2nd order elliptic equations. *Mathematics of Computation*, 31(138):391–413, 1977.

[Russell *et al.*, 2008] Francis P. Russell, Michael R. Mellor, Paul H.J. Kelly, and Olav Beckmann. Desola: An active linear algebra library using delayed evaluation and runtime code generation. *Science of Computer Programming*, In Press, Corrected Proof:–, 2008.

[Seiler *et al.*, 2008] Larry Seiler, Doug Carmean, Eric Sprangle, Tom Forsyth, Michael Abrash, Pradeep Dubey, Stephen Junkins, Adam Lake, Jeremy Sugerman, Robert Cavin, Roger Espasa, Ed Gochowski, Toni Juan, and Pat Hanrahan. Larrabee: a many-core x86 architecture for visual computing. *ACM Trans. Graph.*, 27(3):1–15, August 2008.

[Siek, 1999] J.G. Siek. A modern framework for portable high performance numerical linear algebra. Master’s thesis, University of Notre Dame, 1999.

[SPIRAL Project, 2010] The SPIRAL Project. Benchmarks: Spiral generated programs. <http://www.spiral.net/bench.html>, Retrieved 22 May, 2010.

[Taylor *et al.*, 2007] Zeike A. Taylor, Mario Cheng, and Sébastien Ourselin. Realtime Nonlinear Finite Element Analysis for Surgical Simulation Using Graphics Processing Units. In *In Proceedings of the 10th International Conference on Medical Image Computing and Computer Assisted Intervention (LNCS 4791)*, pages 701–708. Springer Berlin/Heidelberg, 2007.

[Taylor *et al.*, 2008] Z.A. Taylor, M. Cheng, and S. Ourselin. High-Speed Nonlinear Finite Element Analysis for Surgical Simulation Using Graphics Processing Units. *Medical Imaging, IEEE Transactions on*, 27(5):650–663, May 2008.

[Turek *et al.*, 2010] Stefan Turek, Dominik Göddeke, Christian Becker, Sven H.M. Buijssen, and Hilmar Wobker. FEAST – Realisation of hardware-oriented numerics for HPC simulations with finite elements. *Concurrency and Computation: Practice and Experience*, February 2010. Special Issue Proceedings of ISC 2008.

[Veldhuizen, 1998] Todd L. Veldhuizen. Arrays in blitz++. In *ISCOPE '98: Proceedings of the Second International Symposium on Computing in Object-Oriented Parallel Environments*, pages 223–230, London, UK, 1998. Springer-Verlag.

[Vos *et al.*, 2009] Peter E. J Vos, Spencer J. Sherwin, and Robert M. Kirby. From h to p efficiently: implementing finite and spectral/hp element discretisations to achieve optimal performance at low and high order approximations. Submitted to *Journal of Computational Physics*. <http://www2.imperial.ac.uk/ssherw/spectralhp/papers/JCP-VoShKi-09.pdf>, October 2009.

[Vuduc *et al.*, 2005] Richard Vuduc, James W. Demmel, and Katherine A. Yelick. OSKI: A library of automatically tuned sparse matrix kernels. In *Proceedings of SciDAC 2005, Journal of Physics: Conference Series*, San Francisco, CA, USA, June 2005. Institute of Physics Publishing. (*to appear*).

[Vuduc, 2003] Richard W. Vuduc. *Automatic performance tuning of sparse matrix kernels*. PhD thesis, University of California, Berkeley, December 2003.

[Wesseling, 2001] Pieter Wesseling. *Principles of computational fluid dynamics*. Springer, 2001.

[Whaley and Dongarra, 1998] R. Clint Whaley and Jack J. Dongarra. Automatically tuned linear algebra software. In *Supercomputing '98: Proceedings of the 1998 ACM/IEEE conference on Supercomputing (CDROM)*, pages 1–27, Washington, DC, USA, 1998. IEEE Computer Society.

[Whalley, 2005] David B. Whalley. Tuning high performance kernels through empirical compilation. In *ICPP '05: Proceedings of the 2005 International Conference on Parallel Processing*, pages 89–98, Washington, DC, USA, 2005. IEEE Computer Society.

[Zhu *et al.*, 2010] Yun Zhu, Edwin Westbrook, Jun Inoue, Alexandre Chapoutot, Cherif Salama, Marisa Peralta, Travis Martin, Walid Taha, Marcia O’Malley, Robert Cartwright, Aaron Ames, and Raktim Bhattacharya. Mathematical equatinos as executable models of mechanical systems. In *Proceedings of the ACM/IEEE 1st International Conference on Cyber-Physical Systems (to appear)*, April 2010.